

**Prolonged Sulfur Dioxide Degassing at the Soufrière Hills Volcano, Montserrat, and
implications for deep magma permeability**

Thomas Christopher ^{1*}, Marie Edmonds ², Benoit Taisne ³, Henry Odbert ⁴, Antonio Costa ⁵, Victoria
Hards ⁶, Geoff Wadge ⁷

1. Montserrat Volcano Observatory, Salem, Montserrat, West Indies.

2. Department of Earth Sciences, University of Cambridge, Downing Street, Cambridge,
Cambridgeshire UK, CB2 3EQ

3. Earth Observatory of Singapore, Nanyang Technological University, 50 Nanyang Avenue,
N2-01B-25 Singapore 639798

4. School of Earth Sciences, University of Bristol, Wills Memorial Building, Queen's Road, Bristol
BS8 1RJ, UK

5. Istituto Nazionale di Geofisica e Vulcanologia - Sezione di Bologna, Via Donato Creti, 12,
40128 Bologna, Italy Tel: (+39)0816108446

6. British Geological Survey Environmental Science Centre Nicker Hill Keyworth
Nottingham NG12 5GG

7. Environmental Systems Science Centre, University of Reading,
Reading, UK

*corresponding author; Thomas@mvo.ms

Words = 6743 References = 118 Tables = 1 Figures = 9

Abbreviated Title: Prolonged SO₂ degassing at Souf Hills

27 **Abstract**

28 The installation of a network of UV spectrometers on the western flank of the Soufrière Hills
29 volcano has produced a robust dataset of sulfur dioxide fluxes over a thirteen year period (2000-
30 2013). The emission of SO₂ has been quasi-continuous over the course of the eruption which is
31 in contrast to the highly discontinuous eruption of lava. Analysis of the flux time series indicates
32 that a degree of periodicity is present in the SO₂ signal, ranging from hours to years. Previous
33 studies show that pulses in the SO₂ flux of ≤ 50 days can be correlated with other volcanic
34 activity such as seismic activity and extrusion. We identify two longer period signals in the SO₂
35 data, one at ~ 5 months and the other at ~ 2 years, which are independent of lava extrusion and
36 ground deformation. We investigate possible causes of these periodic degassing signals, e.g.
37 hydrological, atmospheric, and magmatic controls. We hypothesize that the trends in the
38 degassing time series are sourced from deeper levels in the volcanic plumbing system, related to
39 deformation of the lower reservoir which brings about localized pressure changes. We also
40 discuss the mechanisms by which the sulfur-rich gases might reach the surface.

41

42 **INTRODUCTION**

43 Understanding volcanic sulfur dioxide (SO₂) degassing processes is an important tool for the
44 monitoring of volcanoes e.g. (Casadevall et al., 1983; Bluth et al., 1994; Fischer et al., 1994;
45 Young et al., 1998a; Aiuppa et al., 2009; Werner et al., 2013). Sulfur emissions from volcanoes
46 have been used to forecast the onset of impending eruptions (e.g. Caltabiano et al., 1994) or to
47 assess the level of activity during an ongoing eruption (e.g. Casadevall et al., 1983; Gerlach and
48 McGee, 1994; Mc Gee and Sutton, 1994; Hirabayashi et al., 1995; Luckett et al., 2002; Zobin et
49 al., 2008; Komorowski et al., 2010). In recent years, long time series of SO₂ emissions have been

50 built owing to recent developments in low-cost automated spectrometer networks which operate
51 in the ultra-violet region of the electromagnetic spectrum, allowing SO₂ fluxes to be measured
52 every few minutes through daylight hours using Differential Optical Absorption Spectroscopy
53 (DOAS; e.g. Edmonds et al., 2003a; Galle et al., 2003; Mc Gonigle et al., 2003). Soufrière Hills
54 Volcano was the first focus of this volcano-monitoring development (Edmonds et al., 2003a;
55 Christopher et al., 2010), and consequently there now exists an unprecedented 18-year long time
56 series of SO₂ emissions, the last 11 years a result of the spectrometer network. Over the course of
57 the eruption, the time series has lent insight into magma supply and eruption processes
58 (Edmonds et al., 2001; Edmonds et al., 2003b; Young et al., 2003; Edmonds et al., 2010;
59 Christopher et al., 2010; Nicholson et al., 2013), and has been used for volcano monitoring and
60 hazard assessment.

61

62 The andesite erupted over the course of the 1995-current eruption exhibits a wealth of
63 disequilibrium features on a range of scales, as well as decimeter-sized mafic enclaves (Murphy
64 et al., 1998; Murphy et al., 2000; Humphreys et al., 2009a; Barclay et al., 2010; Plail et al., in
65 press). The andesite is the result of a complex magma genesis, dominated by magma mixing and
66 fractional crystallization during its long residence in an upper-mid crustal magma reservoir
67 (Murphy et al., 1998; Murphy et al., 2000; Zellmer et al., 2003; Humphreys et al., 2009a; 2009b;
68 Humphreys et al., 2012; Christopher et al., in press), in common with other andesite systems
69 (e.g. Fichaut et al., 1989; Sato et al., 1999; Martel et al., 2006; Kent et al., 2010; Ruprecht &
70 Plank, 2013). The resulting hybrid magma contains ~ 45 vol% phenocrysts of plagioclase,
71 orthopyroxene and hornblende (Murphy et al., 1998; 2000), in a rhyolitic melt.

72

73 The volatile budget of such an open system is likely to be complex. The low concentrations of
74 sulphur in the plagioclase-hosted melt inclusions (<100 ppm, Edmonds et al., 2001) is not
75 sufficient to account for the mass of sulfur degassed during the eruption (which would require
76 melt concentrations of >1000 ppm sulfur; Christopher et al., 2010). This observation of "excess
77 sulfur" is in common with most other oxidized intermediate-silicic volcanic systems worldwide
78 (e.g. Andres et al., 1991; Gerlach & McGee, 1994; Wallace, 2001; Wallace, 2005; Shinohara et
79 al., 2008a; Wallace and Edmonds, 2011). Much of the sulfur in the system exists in the vapour
80 phase prior to magma ascent and eruption, and the vapour is probably replenished by intruding
81 mafic magma, either through second boiling during crystallization at the interface between the
82 two magmas, or by changes in solubility caused by the contrasting temperatures and/or oxygen
83 fugacity (Christopher et al., 2010; Edmonds et al., 2010; Edmonds et al., in press).

84

85 This kind of mechanism for volatile transfer has also been proposed to explain the sulfur budget
86 of Pinatubo (e.g. Westrich & Gerlach, 1992; Wallace & Gerlach, 1994; Kress, 1997) and Unzen
87 (e.g. Sato et al., 2005; Ohba et al., 2008; Shinohara et al., 2008b). The strong partitioning of
88 sulfur into a hydrous vapor is consistent with thermodynamical and experimental studies which
89 suggest that for oxidized silicic melts, the solubility of sulfur is low (Scaillet & Pichavant, 2003;
90 Clemente et al., 2004; Moretti & Papale, 2004).

91

92 The flux of SO₂ gas from the volcano is observed to be variable on a range of timescales. The
93 variability has been attributed to shallow magma permeability during "stick-slip" eruptive
94 behavior (Watson et al., 2000), changes in lava extrusion rate (Young et al., 1998a; Luckett et
95 al., 2002) and over months to years timescales, sealing caused by the precipitation of silica in the

96 conduit and dome between eruptive phases (Edmonds et al., 2003b). Cyclic changes in SO₂ on a
97 timescale of ~50 days have been linked to cyclicity in lava extrusion and seismicity (Luckett et
98 al., 2002; Norton et al., 2002; Loughlin et al., 2010; Nicholson et al., 2013).

99

100 There remains, however, some unanswered questions regarding the emission patterns of volcanic
101 gases from Soufrière Hills, and some features of the dataset that make this eruption unique in our
102 view. The first is that over timescales of months to years, the emission of SO₂ appears to be
103 decoupled from the eruption of lava. In general, as much SO₂ degasses when the volcano is not
104 erupting as when it is erupting. Eruptive pauses last 12 to >24 months, and during these
105 relatively long periods SO₂ fluxes are frequently sustained at levels of >500 t/d for weeks to
106 months. This observation requires some deep-seated permeability or advection of the gas phase
107 to be operating, allowing gas to migrate through crystal-rich andesite at depth. Over the dataset
108 as a whole, there are three long period cycles of SO₂ increase and decrease that bear no obvious
109 relation to the eruptive periods (Figure 1).

110

111 The second, related puzzle is that, in the 18th year of quasi-continuous degassing, and in the
112 absence of volcanic activity since February 2011, it would be a useful exercise to evaluate what
113 sort of degassing signature might herald the end of the eruption. Are the continued high fluxes of
114 SO₂ at the surface (>300 t/d) indicative of continued supply of mafic magma at depth, or is it
115 possible that the long-lived, large magma reservoir might be able to supply gas in the absence of
116 new magma, for this kind of extended period? These questions have important implications for
117 monitoring and hazard. In this paper, we present the full time series of SO₂ data, from July 1995
118 to July 2013. We evaluate the possible controls on the long timescale periodicity in the

119 timescale, including gas scrubbing/hydrological control, modulation by a lava dome, and deep
120 magma supply and convection processes. We then discuss the implications of our model for the
121 longevity of the degassing process after the end of the eruption.

122

123 **ERUPTION OVERVIEW**

124 The Soufrière Hills volcano is an andesitic lava dome complex on the island of Montserrat in the
125 lesser Antilles arc. The current eruption began on the evening of July 18th 1995 with ash venting
126 followed by phreatic explosions over the next weeks and months (Young et al., 1998b;
127 Robertson et al., 2000). Juvenile material arrived at the surface around November 15th 1995
128 (Young et al., 1998b) building the first lava dome of the eruption. The eruption has been
129 characterized by 1-2 years of lava effusion and associated dome growth interrupted by 1-2 year
130 long or less periods of no extrusion. This pattern of eruption is in contrast to the quasi-
131 continuous emissions of SO₂ throughout the eruption (Figure 2).

132

133 The effusive episodes are punctuated by pyroclastic flows generated by dome collapse or
134 vulcanian explosions. Episodes of lava extrusion and dome growth at Soufrière Hills are referred
135 to as phases (numbered I to V) while the periods of no magma production are referred to as
136 pauses. During each period of extrusion, deformation and seismic activity correlates strongly
137 with lava extrusion (Figure 3). The volcanic activity of phases I to V is described in detail
138 elsewhere (e.g. Aspinall et al., 1998; Young et al., 1998b; Miller et al., 1998; Calder et al., 2002;
139 Norton et al., 2002; Sparks & Young, 2002; Herd et al., 2005; Loughlin et al., 2010; Ryan et al.,
140 2010; Wadge et al., 2010).

141 The first three phases of dome building were characterized by extended periods (on the order of
142 20 months) of extrusion and pause (Figures 1, 3). Phases IV and V were much shorter: phase IV
143 was characterized by two separate episodes of low extrusion rates punctuated by explosions, the
144 first in July-August 2008 and the second in December 2008-January 2009 (Komorowski et al.,
145 2010). An approximate volume of $30 \times 10^6 \text{ m}^3$ of andesitic lava was erupted for each episode
146 (Wadge et al., 2010). Phase V was also short lived (early October 2009 till mid February 2010),
147 and was associated with the extrusion of $\sim 70 \times 10^6 \text{ m}^3$ of lava. As was the case with phase IV,
148 Phase V was characterized by sporadic explosive activity during extrusion (Stinton et al., in
149 press).

150

151 **METHODOLOGY FOR THE MEASUREMENT OF SULFUR DIOXIDE FLUX**

152 From July 1995 till December 2001, intermittent SO_2 flux measurements were made with the
153 correlation spectrometer (COSPEC) and have been presented elsewhere (e.g. Gardner et al.,
154 1998, Young et al., 1998b). Traverses with the COSPEC under the plume were done by car, boat
155 and helicopter. A detailed description of the COSPEC technique can be found in Stoiber et al.
156 (1987) and Young et al. (2003). Subsequent to the COSPEC; miniature, low cost ultraviolet
157 (UV) spectrometers were used to obtain SO_2 fluxes. The data are reduced using the Differential
158 Optical Absorption Spectroscopy (DOAS) technique (Platt, 1994). Two automated and
159 telemetered UV spectrometers, coupled with scanning devices, were installed on the western
160 flanks of the Soufrière Hills volcano at Lovers Lane and Brodericks (Figure 2) and they collect
161 spectra continuously during daylight hours, thus providing daily flux measurements with an
162 estimated error of $<35\%$ (Galle et al., 2002; Edmonds et al., 2003a). Details of installation of the
163 network, instrument specifications, spectral evaluation, mass flux calculation, associated errors

164 and other information relating to the Soufrière Hills UV scanning network is described in detail
165 by Edmonds et al. (2003a). The UV network provided a more robust and continuous dataset
166 compared to the COSPEC and has produced a virtually continuous record of SO₂ fluxes for more
167 than 10 years. It must be noted that the error varies on a daily basis in the measurements due to
168 variable conditions and precision is more reliable than accuracy for the flux measurements.

169

170 **THE SULFUR DIOXIDE FLUX TIME SERIES**

171 *Phases I & II / Pauses I & II*

172 Initial degassing measurements were performed at the Soufrière Hills from July 29th 1995 to
173 early September 1995 (Young et al, 1998a; Gardner and White, 2002). The measurements were
174 carried out during the period of early phreatic activity in the eruption, prior to the onset of dome
175 growth. SO₂ fluxes were 300 - 800 t/d and peaked at 1200 t/d on August 6th. The SO₂ emission
176 rate shows a general increase from 1996 to 1997 during the first extrusion phase (Figure 1). The
177 mean daily SO₂ flux during the first extrusion episode was 569 t/d. The highest measured daily
178 output was 4150 t/d on July 13th 1998; this high value followed closely a large dome collapse
179 which occurred on July 3rd 1998 (Norton et al., 2002; Edmonds et al., 2003b). The SO₂ flux
180 showed an overall downward trend during the first pause period with a daily mean of 699 t/d,
181 with a peak value of 4150 t/d occurring on July 13th 1998. From 1997 to mid 1999 (most of
182 phase I and all of pause I), the SO₂ signal is generally defined by large pulsed signal over the
183 duration (Figure 1).

184

185 The SO₂ flux during the Phase II also define pulse like signals over durations of years, the first
186 from late 1999 to mid 2001 which peaked in late August – early September 2000, with a value of
187 2570 t/d (Figure 1). Another SO₂ pulse started in early 2002 and extends into the second pause
188 period. The SO₂ flux during Phase II had a daily mean of 472 t/d. The SO₂ flux during Phase II
189 peaked in early September 2000 (2570 t/d) after which the SO₂ flux decreased until around April
190 2001. This was followed by a general increase in SO₂ flux until the end of the extrusive episode
191 in early August 2003 (Figure 1).

192

193 The mean daily SO₂ flux during the entire second pause was 562 t/d. The general increase in SO₂
194 flux that began during Phase II continued into the second pause period until early September
195 2003 when there was a general decreasing trend until June 2004. The mean daily flux from the
196 start of the pause period until June 2004 was 696 t/d, after which the daily fluxes defined a fairly
197 flat trend (~400 t/d), which continued until April 2005. The mean SO₂ flux over this month was
198 377 t/d. After April 2005, SO₂ flux began increase once again (up to 534 t/d) leading up to the
199 onset of Phase III of lava extrusion (Figure 1). The peak SO₂ flux of the pause period (12,999
200 t/d) occurred on October 8th 2004, during the time when the mean daily flux for the month was
201 otherwise 388 t/d. This is the highest daily mean flux measured during the eruption to date.

202

203 *Phases III & IV / Pauses III, IV and V*

204 The general trend of increasing SO₂ flux from the second pause, continued into Phase III. The
205 SO₂ flux increased up to October 2005 to a maximum flux of 1522 t/d, after which it broadly
206 decreased up until July 2006 after which another period of low flux values (~ 300 t/d) occurred

207 and lasted until July 2007. The mean daily flux for the whole of Phase III is 440 t/d. The peak
208 flux value during Phase III (3980 t/d), occurred on the last day of lava extrusion (April 4th 2007).
209 It must be however noted that the mean daily flux for the first ten days of April 2007 was ~ 2000
210 t/d.

211

212 The SO₂ flux at the start of pause III were elevated over the eruption mean, however the flux
213 decreased again and remained fairly low (274 t/d) until July 2007 when another general increase
214 in the daily flux values began. This increasing trend in SO₂ flux continued until late May 2008;
215 the mean daily flux during this period was 688 t/d. There was another trend of decreasing flux
216 values from mid April 2008 till July 18th 2008, when the SO₂ flux was 412 t/d. This was
217 followed by a significant elevation in the SO₂ flux over the next ten days (1100 t/d) that led up to
218 the vulcanian explosion of July 29th 2008 that heralded the start of Phase IV a (Figures 1, 3).

219

220 The SO₂ flux remained elevated until early October 2008 when SO₂ flux again decreased with
221 time, which continued throughout all of Phase IV a, IV b and their subsequent pauses (Figures 1,
222 3). This decreasing trend was brought to an end by the onset of Phase V when the activity
223 incapacitated the spectrometer network with constant heavy ash fall. The mean daily flux from
224 the onset of Phase IVa to the onset of Phase V is 675 t/d. The mean daily flux for Phase IVa is
225 923 t/d while the mean daily for Phase IV b is 451 t/d, which is consistent with a trend of waning
226 daily flux. Flux measurements resumed in mid March 2010 and since then there has been no new
227 lava production at the volcano (Figures 1, 3). The mean daily flux between March 17th 2010 and

228 August 31st 2010 was ~ 400 t/d and has remained fairly constant (+/- 281 t/d), (Figures 1, 3).

229 Over the entire eruption, the mean daily SO₂ flux has been ~ 500 t/d.

230

231 The SO₂ flux time series clearly show three pulses on time scales of 1.5-3 years (Table 1). The
232 amplitude of the pulses are (200-300 t/d) above the background of 300-400 t/d. The third and
233 most recent pulse had a longer period and higher amplitude than the previous two. Pulses on this
234 timescale appear to have ceased in early 2010, coincidental with the end of Phase V. The mean
235 daily SO₂ output since then is similar to that of the periods intermediate between pulses.

236 Superimposed on these pulses that lasts 2-3 years are shorter timescale variability in the SO₂
237 signal on the order of days to months which is less systematic and appears better correlated with
238 other volcanological phenomena such as lava extrusion and seismicity , volcano-tectonic (VT)
239 earthquakes in particular, which have been occurring since 2007 in short intense bursts lasting
240 less than 1 hour and are referred to as VT strings (Figure 4). VT strings are defined as a short
241 intense swarm of VT earthquakes lasting less than one hour, occurring during a low background
242 level of VT activity with four or more triggered events (Cole et al., 2010).

243

244 **TIME SERIES ANALYSIS**

245 Volcanic SO₂ flux time series typically contain error-induced noise that makes it difficult to
246 recognize and constrain periodicities without a statistical analysis. The time series presented here
247 also contains significant gaps that render statistical analysis by simple Fourier Transform
248 methods non-effective. Degassing time series datasets obtained from volcanoes have been
249 analyzed by wavelet analysis previously and have proven very useful in constraining

250 periodicities in volatile fluxes that relate to episodic volatile delivery (e.g. Oppenheimer et al.,
251 2009; Boichu et al., 2010).

252

$$253 \int_{-\infty}^{\infty} |\psi(t)|^2 dt = 1 \quad (1)$$

254

255 Wavelet analysis decomposes a time series into time–frequency space, thus making it possible to
256 determine both the dominant modes of variability and how those modes vary in time (Torrence
257 & Compo, 1998). Wavelet transforms are mathematical techniques, based on group theory and
258 square integrable representations, which allows unfolding of a signal into both space and scale,
259 by using analyzing functions called wavelets, which are localized in space (Farge, 1992). A
260 wavelet is a wave-like oscillation whose amplitude changes from zero to some maximum then
261 back to zero, or in other words decays over a finite duration.

262

$$263 \int_{-\infty}^{\infty} \psi(t) dt = 0 \quad (2)$$

264

265 This is mathematically achieved by imposing two restrictions on the wavelet function $\psi(t)$.
266 Equation (1) shows that the wavelet function must depart from zero for a limited duration while
267 equation (2) requires a matching negative departure, thus creating a small wave. Generally,
268 wavelets are crafted purposefully to have relevant properties that make them useful for
269 processing a specific signal. The term wavelet function is generally used to refer to either
270 orthogonal or nonorthogonal wavelets.

271 The nonorthogonal transform is useful for time series analysis, where smooth, continuous
272 variations in wavelet amplitude are expected and hence this is the type of wavelet function
273 employed in this study. A nonorthogonal wavelet function can be used with either the discrete or
274 the continuous wavelet transform (CWT) (Farge 1992). Thus the continuous wavelet transform
275 offers a continuous and redundant unfolding in terms of both space and scale.

276

$$277 \quad \psi(t) = \pi^{-1/4} e^{i\omega_0 t} e^{-t^2} / 2 \quad (3)$$

278

279 Wavelet transforms have the advantage of being able to analyze a time series with multiple
280 embedded signals. A Morlet wavelet is a symmetrical (CWT), comprising of an exponential
281 carrier wave modulated by a Gaussian function, equation (3). The Morlet wavelet has the added
282 ability to distinguish components of a time series as they change with time at differing scales.
283 The scale decomposition is obtained by dilating or contracting the chosen analyzing wavelet
284 before convolving it with the signal (Farge 1992).

285

286 The limited spatial support of wavelets is important because then the behavior of the signal at
287 infinity does not play any role. Therefore the wavelet analysis or syn-thesis can be performed
288 locally on the signal, as opposed to the Fourier transform, which is inherently nonlocal due to
289 the space-filling nature of the trigonometric functions (Farge 1992; Percival & Walden, 2000).

290

291

292

293

294 *Wavelet results*

295 The wavelet analysis was applied to the entire dataset after running the data through an 11-day
296 median filter. Gaps in the time series were filled using random values from a population with the
297 same standard deviation as the data. For the wavelet analysis of such a random series, white
298 noise does not exhibit any cycles and hence produces gaps in the plot. The plots generated by the
299 wavelet analysis (Figure 5) confirm that there are two cycles in excess of 50 days: one at ~ 4-5
300 months and the other in the range ~ 2-3 years, with both being present throughout the entire SO₂
301 time series and are independent of magma extrusion (Figures 1 & 6).

302

303 Nicholson et al. (2013) identified cyclicity on time scales on the order of 2-3 years, 6-8 weeks
304 (50 days) and 10-14 days. Their Fourier Transform methods used for time series analysis differs
305 somewhat from our own. The gaps less than 14 days in the dataset were filled using linear
306 interpolation, however they employed reconstructive analysis methods to account for the larger
307 gaps. And a Short term Fourier Transform (STFT) was employed; a sliding window of spectral
308 snapshots over a specified duration, with each snapshot having varying degrees of overlap with
309 its neighbors. Window lengths of 256-128 days and overlaps of 50% to 99% were used.

310

311 **DISCUSSION**

312 In this section we explore the controls on the 4-5 months and the ~ 2-3 year periodicity in the
313 SO₂ time series. We consider shallow controls: changes in the degree of scrubbing of SO₂ from
314 the gases on long cycles controlled by changes in the groundwater level or other hydrological

315 factors; and changes in the shallow permeability of the conduit and lava dome (i.e. "open vent"
316 conditions might promote high gas fluxes, the presence of a lava dome might subdue
317 outgassing). We then consider deeper controls: the sulfur is thought to be linked ultimately to the
318 supply of mafic magma at depth (e.g. Edmonds et al., 2001; 2010).

319

320 Models of ground deformation suggest there are two linked magma reservoirs, one at ~6 and one
321 at ~12 km depth (Elsworth et al., 2008; Foroozan et al., 2010; Paulatto et al., 2010; Foroozan et
322 al., 2011). Dual reservoirs feeding silicic volcanoes have been proposed elsewhere: Tomiya et
323 al. (2010) put forward petrological evidence for a dual reservoir configuration beneath Mt Usu
324 volcano in Japan. The depth at which the mafic magma interacts with the andesite is however not
325 well constrained thus while the SO₂ flux at the surface may be a proxy for deep magma supply,
326 there is likely to be a time lag for S-rich vapour to escape from the system through a large body
327 of crystal-rich andesite.

328

329 During eruptive periods magmatic vapour is advected by upward-moving magma and augmented
330 by syn-eruptive degassing, which can be clearly seen in the correlations between lava extrusion
331 rate, seismicity and SO₂ flux recorded previously (e.g. Gardner and White, 1998; Young et al.,
332 1998; Watson et al., 2000; Young et al., 2003; Nicholson et al., 2013). However, SO₂ outgassing
333 during periods of no magma extrusion (pauses) are clearly not advected by moving magma. In
334 this case it must migrate through a crystal-rich andesitic magma body to the surface.

335

336 We therefore investigate the characteristic time scales for a batch of gas to move through a large
337 andesite magma body. We also explore the possibility that the mafic magma body is convecting
338 at depth, and perturbations as a result of this convection might give rise to cyclic degassing. And
339 lastly we explore the timescales of magma convection in a crystal-rich andesite using existing
340 models (Kazahaya et al., 1994; Stevenson & Blake, 1998; Couch et al., 2001).

341

342 *Metrological /Aquifer control*

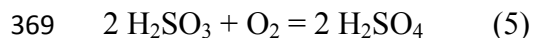
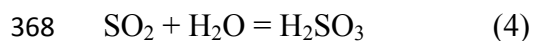
343 It has been shown that the abundance of SO₂ in volcanic plumes can be influenced by
344 groundwater aquifer levels, the hydrothermal system and atmospheric humidity, in a process
345 referred to as scrubbing (e.g. Doukas & Gerlach, 1992; Sutton et al., 1997; Symonds et al., 2001;
346 Gerlach et al., 2002; Duffell et al., 2003; Werner et al., 2006; Rodriguez et al., 2008; Werner et
347 al., 2012). Scrubbing involves the chemical interaction of SO₂ in the volcanic plume with water
348 and oxygen, described in equations 4 and 5. The interaction of SO₂ with H₂O yields the
349 hydrolysis reaction in equation 4, which results in the reduction of SO₂ and the formation of
350 hydrosulfuric acid (H₂SO₃), an inherently weak acid. This can be further oxidized to form mild
351 sulfuric acid (H₂SO₄) although this is slow process.

352

353 Scrubbing at the Soufrière Hills Volcano has been shown to account for SO₂ loss rates exceeding
354 10⁻³ s⁻¹ (Oppenheimer et al., 1998), with a mean of 10⁻⁴ s⁻¹ (Rodriguez et al., 2008). The
355 spectrometers typically measure the plume within 5 minutes of the gas being emitted from the
356 vent, and so using these loss rates we estimate that scrubbing might account for a typical
357 underestimate of up to 70% of the SO₂ degassing from the vent (Rodriguez et al., 2008).

358 The loss rate of SO₂ might vary between the wet and the dry season. The relative humidity is
359 heavily dependent on the rainy season, which coincides with the Atlantic hurricane season and
360 thus varies sub-annually. This variation in humidity through the year might explain the
361 differences in loss rates obtained by the afore-mentioned studies (Oppenheimer et al., 1998;
362 Rodriguez et al., 2008). Increased rainfall would thus act to lower the SO₂ abundance in the
363 plume by scrubbing either in the subsurface hydrothermal system or in the atmosphere.
364 Oppenheimer et al. (1998) performed their measurements, finding the highest loss rates, during
365 the peak of the rainy season when the relative humidity would be highest for the year while
366 Rodriguez et al. (2008) performed their measurements on ash-free plumes during the dry season.

367



370

371 SO₂ might also be removed prior to outgassing, in a subsurface hydrothermal system.
372 Geochemical studies the early 1990s revealed the existence of a large hydrothermal/geothermal
373 system in the entire southern portion of the island, beneath the Soufrière Hills volcano (Chiodini
374 et al., 1996). The hot springs in Soufrières (fumaroles) on the flanks of the volcano prior to the
375 onset of the current eruption contained sulfate and chloride species, indicative of dissolution of
376 magmatic gases into the water (Chiodini et al., 1996). Cold spring outputs on Montserrat are
377 directly correlated with the groundwater levels. The rainy season coincides with the Atlantic
378 hurricane season and thus the 5 month pulsation might be modulated by the change in rainfall. A
379 comparison of the monthly output of two proximal springs over the same duration as the SO₂

380 dataset from the spectrometer network (Figure 7) shows no correlation between the datasets and
381 we therefore reject control by the hydrothermal/geothermal system as a primary control on the
382 SO₂ flux periodicity on 5 month timescales.

383

384 *Dome-modulated gas storage or release*

385 Dome collapses and explosions at the Soufrière Hills volcano are frequently accompanied by
386 releases of large quantities of SO₂ (e.g. Herd et al., 2005; Carn & Prata, 2010; Komorowski et
387 al., 2010). Lava domes may trap volatiles in the shallow plumbing system by loading the
388 volcanic edifice, causing the closing of fractures around the volcanic conduit which inhibits
389 volatile leakage, the effectiveness of which is dependent on the dome height and foot print
390 (Woods and Huppert, 2003; Taisne & Jaupart, 2008). A wider and higher dome is more efficient
391 at loading the edifice and thus acts to reduce SO₂ outgassing.

392

393 There is no detailed data regarding the width of the base of the lava dome; however the 1 km
394 diameter crater puts constraints on the dome foot print, and there have been a number of
395 occasions when the base of the dome has filled the entire crater, for example during extrusion
396 phase II (late May 2002 till July 2003) and also in Phase III from February 2007 to April 2007
397 the dome had a volume of $\sim 200 \times 10^6 \text{ m}^3$ which is the largest to date (Ryan et al., 2010; Wadge et
398 al., 2010). The large dome persisted through the next pause period and through extrusive Phases
399 IV and V, with a net volume of $38 \times 10^6 \text{ m}^3$ of lava added to the dome during both episodes
400 (Stinton et al., in press).

401

402 The dome height was >1000 m a.s.l on April 4th 2007 (Ryan et al., 2010) and has been
403 consistently greater than this since, particularly during Phase V (Stinton et al., in press). The low
404 SO₂ flux during late 2006 and early 2007 is consistent with a dome-modulated SO₂ signal.
405 However, the dome has had a volume of ~ 200 x 10⁶ m³ and a height of > 1000 m a.s.l since
406 2007, yet another pulse of SO₂ occurred from June 2007 till Jan 2010, during a period when of
407 one of the largest emplaced domes of the eruption was present in the crater (Wadge et al., 2010;
408 Figure 8).

409

410 Thus the size of the lava dome may not be exerting a first order control on SO₂ flux. In mid-
411 2003 the SO₂ flux was increasing contemporaneously with an increasing dome volume and
412 height (Figure 8). The highest extrusion rates during the eruption occurred in early 2006 leading
413 up to the May 20th 2006 collapse and also during Phase V. Both these periods coincide with a
414 waning SO₂ flux (Figure 9), which is contrary to what you would expect for a first order control
415 since increased extrusion rates should enhance degassing at the surface. Conversely the general
416 trend of increasing SO₂ fluxes observed between Phases III and IV occurred during a period of
417 no lava extrusion. Thus as is the case with the dome volume, there is also no correlation between
418 the SO₂ and andesite extrusion rate (Figure 9). We therefore propose that the 1.5-2.5 year pulses
419 in the SO₂ signal are neither modulated by the lava dome or extrusion rate.

420

421 *SO₂ origin and degassing timescales*

422 Petrological work on the eruptive products of Phase I showed that the enclaves and mafic
423 groundmass are indicative of the intrusion of mafic magma, which may trigger and fuel the

424 eruption (e.g. Barclay et al., 1998; Murphy et al., 1998; Murphy et al., 2000; Devine et al., 2003).
425 Melt inclusions hosted by plagioclase contain very little sulfur (Edmonds et al., 2001), certainly
426 not enough to account for the large fluxes of SO₂ outgassing at the surface. Hence the andesite
427 residing in the Soufrière Hills reservoir is thus thought to be in equilibrium with a significant
428 exsolved gas phase (e.g. Anderson, 1975; Gerlach, 1994; Wallace, 2001; 2005; Edmonds et al.,
429 2008; Wallace & Edmonds, 2011; Witham, 2011).

430

431 The intruding mafic magma almost certainly supplies heat and volatiles to the overlying andesite,
432 by a process similar to either gas sparging (e.g. Bachman & Bergantz., 2006; 2008) where the
433 gases act as a “defrosting” agent, transferring heat to the overlying silicic magma (e.g. Bachman
434 & Bergantz., 2003), the development of volatile-rich melt plumes at the interface (.e.g. Philips &
435 Woods, 2002) or during second boiling which is caused by quench crystallization at the basalt –
436 andesite interface (e.g. Martin et al., 2006; Edmonds et al., in press).

437

438 There is evidence, from e.g. diffusion profiles in Fe-Ti oxides (Devine et al., 2003) and the
439 preservation of the K₂O-rich heterogeneities interpreted to be due to mafic intrusion and
440 diffusive mixing (Humphreys et al., 2010) that the time scale between intrusion, heating of the
441 andesite, quench-driven degassing and eruption of the hybrid magmas is on the order of hours to
442 months. Patterns of ground deformation (Figure 3) reflect the eruption of andesite at the surface
443 (periods of deflation accompanying eruption) and recharge of mafic magma (inflation during
444 eruptive pauses) (e.g. Voight et al., 1999; Elsworth et al., 2008; Foroozan et al., 2011). The SO₂
445 pulses do not exhibit a correlation with ground deformation (Figure 3) indicating that there is no

446 first order control by the intrusion of magma at depth on the long cycles in the SO₂ flux at the
447 surface.

448

449 *CYCLIC ACTIVITY AT Soufrière Hills AND AT OTHER LAVA-DOME BUILDING ERUPTIONS*

450 Cyclic lava extrusion and or degassing displaying periodicities on several different time scales is
451 well documented at a number of different type of volcanoes (e.g. Denlinger & Hoblitt, 1999;
452 Voight et al., 1999; Voight et al., 2000; Barmin et al., 2002; Harris & Neri, 2002; Sparks &
453 Young, 2002; Lazute et al., 2004; Harris et al., 2005; Sweeney et al., 2008; Oppenheimer et al.,
454 2009; Wadge et al., 2010; Melnik & Costa, in press) and pulsations in magma discharge rates
455 appears to be characteristic of dome-building eruptions (Barmin et al., 2002).

456

457 Cyclic patterns in lava effusion and SO₂ emissions were evident from the onset of and has
458 characterized the Soufrière Hills eruption (e.g. Miller et al., 1998; Young et al., 1998; Voight et
459 al., 1998; 1999; Roberston et al., 2000; Lensky et al., 2008; Loughlin et al., 2010). For example,
460 Voight et al. (1998) identified a 6–14 h inflation cycle caused by magma pressurization at
461 shallow depths (< 0.6 km below the base of dome) during the first episode of dome building
462 (Phase I), which was related to non-linear dynamics of magma flow with stick-slip flow (e.g.
463 Denlinger & Hoblitt, 1999; Voight et al., 1999). Druit et al. (2002) reported cycles (10 hour
464 mean) in the vulcanian explosions of 1997 at the Soufrière Hills.

465

466 Sparks & Young (2000) identified a 6 to 7 week magma extrusion cycle in 1997 while Loughlin
467 et al. (2010) also showed that there was a two to six week pulsed signal in the magma discharge
468 rate during Phase III. More recently in Phase V, magma delivery to the surface occurred in three

469 major pulses ranging from 30-45 days duration (Stinton et al., in press), with sub-daily cycles on
470 the order or 4-14 hours (Odbert et al., in press). Odbert et al., (in press) further showed that
471 cyclic behavior at the Soufrière Hills volcano can range from sub-daily (hours) to multi-decadal.
472 It is not uncommon to encounter multiple superimposed cycles hence a single explanation will
473 not be satisfactory since multiple processes are likely involved (Costa et al., 2007). It has been
474 shown by many recent studies that pulsed out flux can exist in a system with a constant influx of
475 magma into a magma reservoir (Melnik & Sparks, 1999; Melnik & Sparks, 2002; Barmin et al.,
476 2002, Melnik & Costa, in press).

477

478 A number of models exist that explain how the none-continuous delivery of lava to the surface
479 throughout the Soufrière Hills eruption . The models employ the nonlinear effects of
480 crystallization and gas loss which leads to rheological stiffening, and pressurization (e.g.
481 Melnik & Sparks, 1999; Voight et al., 1999). Rheological stiffening increases magma
482 overpressure (Melnik & Sparks, 2002), changes in magma pressure and crystallization kinetics
483 causes a strong feedback mechanism and multiple steady solutions for discharge rate (Melnik &
484 Sparks, 2002). Large changes in discharge rate and eruptive behavior can occur as the
485 consequence of small changes in chamber pressure thus promoting none linear extrusion of
486 magma at the surface (Melnik & Sparks, 2002). The system can thus fluctuate between low and
487 high discharge rates at the surface (Melnik & Sparks, 2005).

488

489 Stick-slip magma flow in the upper conduit might result from degassing-induced changes in
490 crystal content and hence bulk viscosity of the magma (Sparks & Young 2002; Sparks, 2003)
491 When the magma overpressure drops to the dynamic strength of the slip surfaces, the plug sticks

492 and blocks the vent thus initiating another episode of increasing magma pressure and another
493 eruptive cycle (Lensky et al., 2008). Costa et al. (2007) proposed a model for the 6- 7 week
494 cycles and attributed it to the elastic deformation of the dyke which connects the upper reservoir
495 to a conduit that leads to the surface, the dyke behaves like a capacitor that deforms and stores
496 magma eventually releasing it when the pressure increases to an optimum value.

497

498 Pulsed lava effusion is documented for the Mt St Helens (1980-1987) eruption and the
499 Santiaguito (1922-2000) eruption. Barmin et al. (2002) used a mathematical model to describe
500 the pulsatory behavior of Mt St Helens, which incorporates the non-linear response to magma
501 extrusion to chamber pressure, owing to the changes in rheological properties and development
502 of overpressures during degassing and ascent (Melnik and Sparks, 1999; Melnik and Sparks,
503 2002; Slezin, 2003). They showed that for a fixed chamber pressure, three different magma
504 ascent velocities can occur. For a steady magma influx, decreases in conduit diameter, crystal
505 growth rate and crystal number density in the magma can generate periodic behavior.

506

507 Elsworth et al. (2008) suggests a fairly steady and continuous influx of mafic magma into the
508 lower reservoir with a flux rate in the range of $(1.2-2.0) \text{ m}^3\text{s}^{-1}$ (Foroozan et al., 2011; Melnik &
509 Costa, in press). The short timescales between reheating and extrusion (e.g. Devine et al., 2003;
510 Rutherford & Devine 2003) indicate that basalt influx into the andesite reservoir and the
511 extrusion of andesite are correlated in time and likely occur for similar durations, this is
512 consistent with the model of Melnik & Costa (in press) where influx of fresh magma into the
513 andesite reservoir results in dome extrusion. The short term pulsations in the SO_2 signal, < 50
514 days (Nicholson et al., 2013) that can be correlated with seismic phenomena (e.g. Luckett et al.,

515 2002; Norton et al., 2002; Loughlin et al., 2010) are likely driven by the shallower and smaller
516 andesite reservoir.

517

518 The duration of the effusion phases have however decreased since 2007, suggesting variability in
519 one or more parameters relevant for modulating oscillatory periods of the lava effusion. We did
520 mention that the duration of the SO₂ pulses are similar to that of the first three extrusion episodes
521 and the last pulse occurred just after the nature of the extrusion changed. It would thus be also
522 fair to conclude that the durations of the initial three extrusion phases and the durations of the
523 pulses in the SO₂ signal are not coincidental.

524

525 *Reservoir connectivity model*

526 Barmin et al. (2002) showed that lava extrusion rate can be variable at constant pressure in the
527 andesite reservoir; however we have demonstrated that the SO₂ pulses are not being controlled
528 by the andesite reservoir. Recent geophysical studies (e.g. Foroozan et al., 2010, Melnik &
529 Costa, in press) have shown that the deformation signal which correlates with extrusion at the
530 Soufrière Hills (Figure 3) can be attributed to both reservoirs. Melnik and Costa, (in press)
531 assumed a steady influx into the deep chamber and used numerical modeling to show that both
532 reservoirs are deforming and the level of connectivity between the two reservoirs are via an
533 elastic dyke determines how much of an influence the deformation of the lower reservoir has on
534 the signal at the surface at any time during the deformation cycle in Figure 3. Thus connectivity
535 between the reservoirs at any point in time is dependent on the dyke width.

536

537 Variations in the connectivity of the reservoirs can also influence the pressure within each
538 reservoir and the dyke. When the connectivity is weak the overpressure in the deep reservoir
539 reaches high values (~ 70 MPa) and remains fairly constant during the cycle and the influx of
540 fresh magma into the shallow reservoir is also nearly constant, high chamber overpressure
541 influences the horizontal extension of the dyke and a consequent improvement of connectivity
542 between two magma chambers. For a strong connectivity between the chambers their
543 overpressures increases or decreases during the cycle in a synchronous way. Influx into the
544 shallow chamber stays close to the extrusion rate at the surface.

545

546 Though the solubility of sulphur solubility is not mainly controlled by pressure (e.g. Scaillet et
547 al., 1998; Scaillet & Pichavant, 2005) there is no petrological evidence indicating systematic
548 changes in melt composition, temperature, fO_2 and fS_2 that correlate with the SO_2 pulses. We
549 therefore propose that the (1.5- 2.5 year) pulses in SO_2 are related to localized pressure changes
550 in the lower reservoir or dyke. The similarity in duration of the first three extrusion phases with
551 the SO_2 pulses is consistent with the driving mechanism for both being similar.

552

553 *Conclusions*

554 We have used statistical techniques to demonstrate that like with magma production, there are
555 pulsations in the SO_2 signal that vary on times scales of months to years. The pulses are
556 however not correlated with extrusion which makes interpretation a bit tedious. We have
557 however being able to rule out processes such as meteorological and aquifer control for
558 controlling the SO_2 signal. We have also ruled out modulation by the lava dome. We therefore
559 rely on the already established geophysical models of (Foroozan et al., 2010, Melnik & Costa,

560 in press) which established the presence of two reservoirs and how they physically interact with
561 each other given a certain degree of connectivity. We therefore embrace the model of (Melnik &
562 Costa, in press) where pressure changes occur in the lower reservoir and connecting dyke that
563 can influence sulfur solubility in the resident magma.

564

565

566

567

568

569

570

571

572

573

574

575

576

577

578

579

580

581

582

583

584

References

585

586 AIUPPA A., FEDERICO C., GIUDICE G., GIUFFRIDA G., GUIDA R., GURRIERI S., LIUZZO M.,
587 MORETTI R. & PAPALE P. 2009. The 2007 eruption of Stromboli volcano. Insights from real-
588 time measurement of the volcanic gas plume CO₂/SO₂ ratio. *Journal of Volcanology and*
589 *Geothermal Research*. **182**(3-4), 221-230.

590

591 ANDRES R.J., ROSE W.I., KYLE P.R., DESILVA S., FRANCIS P., GARDEWEG M. & MORENO ROA
592 H. 1991. Excessive sulfur dioxide emissions from Chilean volcanoes. *Journal of Volcanology*
593 *and Geothermal Research* **46** (3-4), 323-329.

594

595 ASPINALL W. P., MILLER A. D., LYNCH L. L., LATCHMAN J. L., STEWART R. C., WHITE, R. A &
596 POWER J. A. 1998. Soufrière Hills Eruption, Montserrat, 1995-1997. Volcanic earthquake
597 locations and fault plane solutions. *Geophysical Research Letters* **25** (18), 3397-3400.

598

599

600 BACHMANN O. & BERGANTZ G.W. 2003. Rejuvenation of the Fish Canyon magma body: A
601 window into the evolution of large-volume silicic magma systems
602 10.1130/G19764.1 *Geology* **31** (9), 789-792

603

604 BACHMANN O. & BERGANTZ G.W. 2006. Gas percolation in upper-crustal silicic crystal mushes
605 as a mechanism for upward heat advection and rejuvenation of near-solidus magma bodies.
606 *Journal of Volcanology and Geothermal Research* **149**(1-2), 85-102.

607

608 BACHMANN O. & BERGANTZ G.W. 2008. Deciphering Magma Chamber Dynamics from Styles of
609 Compositional Zoning in Large Silicic Ash Flow Sheets. *Reviews in Mineralogy and*
610 *Geochemistry* **69** (1), 651-674

611

612 BARCLAY J., RUTHERFORD M.J., CARROLL M.R., MURPHY M.D., DEVINE J.D., GARDNER J. &
613 SPARKS, R.S.J. 1998. Experimental phase equilibria constraints on pre-eruptive storage
614 conditions of the Soufriere Hills magma. *Geophysical Research Letters* **25**(18), 3437-3440.

615

616 BARCLAY J., HERD R. A., EDWARDS B. R., CHRISTOPHER T.E., KIDDLE E. J., PLAIL M. &
617 DONOVAN A. 2010. Caught in the act: Implications for the increasing abundance of mafic
618 enclaves during the recent eruptive episodes of the Soufrière Hills Volcano, Montserrat.
619 *Geophysical Research Letters* **37**, L00E09, doi:10.1029/2010GL042509.

620

621 BARMIN A., MELNIK O. & SPARKS R.S.J. (2002). Periodic behavior in lava dome eruptions.
622 *Earth and Planetary Science Letters* **199**(1-2), 173-184.

623

624 BLUTH G.J.S., CASADEVALL T.J., SCHNETZLER C.C., DOIRON S.D., WALTER L.S., KRUEGER A.J.
625 & BADRUDDIN M. (1994). Evaluation of Sulfur-Dioxide Emissions from Explosive Volcanism -
626 the 1982-1983 Eruptions of Galunggung, Java, Indonesia. *Journal of Volcanology and*
627 *Geothermal Research* **63**(3-4), 243-256.

628

- 629 BOICHU M., OPPENHEIMER C., TSANEV V. & KYLE P.R. 2010. High temporal resolution SO₂
630 flux measurements at Erebus volcano, Antarctica. *Journal of Volcanology and Geothermal*
631 *Research* **190**(3-4), 325-336.
- 632
633 CALDER E.S., LUCKETT R., SPARKS R.S.J. & VOIGHT B. 2002. Mechanisms of lava dome
634 instability and generation of rockfalls and pyroclastic flows at Soufrière Hills Volcano,
635 Montserrat. *Geological Society, London, Memoirs* **21** (1), 173-190
- 636
637 CALTABIANO T., ROMANO R. & BUDETTA G. 1994. SO₂ flux measurements at Mount Etna
638 (Sicily). *Journal of Geophysical Research*. **99**(D6), 12809-12819.
- 639
640 Carn S.A. & Prata F.J. 2010. Satellite-based constraints on explosive SO₂ release from Soufriere
641 Hills Volcano, Montserrat. *Geophysical Research Letters* **37**. doi: 10.1029/2010GL044971
- 642
643 CASADEVALL T., ROSE W., GERLACH T., GREENLAND L.P., EWERT J., WUNDERMAN R. &
644 SYMONDS R. 1983. Gas Emissions and the Eruptions of Mount St. Helens through 1982. *Science*
645 **221**(4618), 1383-1385.
- 646
647 CHIODINI G., CIONI R., FRULLANI A., GUIDI M., MARINI L., PRATI F. & RACO B. 1996. Fluid
648 geochemistry of Montserrat Island, West Indies. *Bulletin of Volcanology* **58** (380-392).
- 649
650 CHRISTOPHER T., EDMONDS M., HUMPHREYS M.C.S. & HERD R.A. 2010. Volcanic gas
651 emissions from Soufriere Hills Volcano, Montserrat 1995-2009, with implications for mafic
652 magma supply and degassing. *Geophysical Research Letters* **37**. L00E04, doi:
653 10.1029/2009GL041325.
- 654
655 CHRISTOPHER T., HUMPHREYS M.C.S., BARCLAY J., GENAREAU K., De ANGELIS S.M.H., PLAIL
656 M. & DONOVAN A. 2012. Petrological and Geochemical Variation during the Soufrière Hills
657 Eruption (1995-2010). *Geological Society of London Memoir*, eds. G. Wadge, R. Robertson, B.
658 Voight, The eruption of Soufrière Hills Volcano, Montserrat from 2000 to 2010.
- 659
660 COLE P., BASS V., ELIGON C., MURREL C., ODBERT H., SMITH P., STEWART R., STINTON A.,
661 SYERS R., ROBERTSON R. & WILLIAMS P. Report to the Scientific Advisory Committee on
662 Volcanic Activity at Soufriere Hills Volcano Montserrat. Report on Activity between 28
663 February 2010 and 31 October 2010 Open File Report OFR 10-02a
- 664
665 COSTA A., MELNIK O., SPARKS R.S.J. & VOIGHT B. 2007. Control of magma flow in dykes on
666 cyclic lava dome extrusion. *Geophysical Research Letters* **34**(2). doi: 10.1029/2006GL027466
- 667 COUCH S., SPARKS R. & CARROLL M. 2001. Mineral disequilibrium in lavas explained by
668 convective self-mixing in open magma chambers. *Nature* **411** (1037-1039).
- 669
670 DENLINGER, R.P. & HOBLITT, R.P. 1999. Cyclic eruptive behavior of silicic volcanoes. *Geology*
671 **27**(5), 459-462.
- 672

- 673 DEVINE J.D., RUTHERFORD M.J., NORTON G.E. & YOUNG S.R. 2003. Magma Storage Region
674 Processes Inferred from Geochemistry of Fe - Ti Oxides in Andesitic Magma, Soufrière Hills
675 Volcano, Montserrat, W.I. *Journal of Petrology* **44**(8), 1375-1400.
676
- 677 DOUKAS M.P. & GERLACH T. 1992. Sulfur dioxide scrubbing during the 1992 eruptions of
678 Crater Peak, Mount Spurr volcano, Alaska. *The 1992 eruptions of Crater Peak vent, Mount*
679 *Spurr volcano, Alaska* (ed. T. E. C. Keith). US Geol. Surv. Bull. **2139**, 47-57.
680 .
- 681 DRUITT T. H., YOUNG S. R., BAPTIE B., BONADONNA C., CALDER E. S., CLARKE A. B., COLE P.
682 D., HARFORD C. L., HERD R. A., LUCKETT R., RYAN G. & VOIGHT, B. 2002. Episodes of cyclic
683 Vulcanian explosive activity with fountain collapse at Soufriere Hills Volcano, Montserrat.
684 *Geological Society, London, Memoirs* **21**(1). 281-306
685
- 686 EDMONDS M., PYLE D. & OPPENHEIMER C. 2001. A model for degassing at the Soufriere Hills
687 Volcano, Montserrat, West Indies, based on geochemical data. *Earth and Planetary Science*
688 *Letters* **186**(2), 159-173.
689
- 690 EDMONDS M., HERD R.A., GALLE B. & OPPENHEIMER C.M. 2003. Automated, high time-
691 resolution measurements of SO₂ flux at Soufriere Hills Volcano, Montserrat. *Bulletin of*
692 *Volcanology* **65**(8), 578-586.
693
- 694 EDMONDS M., OPPENHEIMER C., PYLE D.M., HERD R.A. & THOMPSON G. 2003. SO₂ emissions
695 from Soufriere Hills Volcano and their relationship to conduit permeability, hydrothermal
696 interaction and degassing regime. *Journal of Volcanology and Geothermal Research* **124**(1-2),
697 23-43.
698
- 699 EDMONDS M., AIUPPA A., HUMPHREYS M., MORETTI R., GIUDICE G., MARTIN R.S., HERD R.A.
700 & CHRISTOPHER T. 2010. Excess volatiles supplied by mingling of mafic magma at an andesite
701 arc volcano. *Geochemistry Geophysics Geosystems* **11** (4). doi: 10.1029/2009GC002781
702
- 703 EDMONDS M., HUMPHREYS M.C.S., HARUI E., HERD R., WADGE G., RAWSON H., LEDDEN R.,
704 PLAIL M., BARCLAY J., AIUPPA A., CHRISTOPHER T., GIUDICE G. & GUIDA R. 2014. Pre-eruptive
705 vapour and its role in controlling eruption style and longevity at Soufrière Hills Volcano.
706 *Geological Society of London Memoir*, eds. G. Wadge, R. Robertson, B. Voight, The eruption of
707 Soufrière Hills Volcano, Montserrat from 2000 to 2010.
708
- 709 ELSWORTH D., MATTIOLI G., TARON J., VOIGHT B. & HERD R. 2008. Implications of Magma
710 Transfer Between Multiple Reservoirs on Eruption Cycling. *Science* **322** (246-248)
711
- 712 FARGE M. (1992). Wavelet Transforms and Their Applications to Turbulence. *Annual Review of*
713 *Fluid Mechanics* **24** (395-457).
714
- 715 FICHAUT M., MARCELOT G. & CLOCCHIATTI R. 1989. Magmatology of Mt. Pelée (Martinique,
716 F.W.I.). II: petrology of gabbroic and dioritic cumulates. *Journal of Volcanology and*
717 *Geothermal Research* **38**(1-2), 171-187.

- 718 Fischer T.P., Morrissey M.M., Calvache M.L., Gomez D., Torres R., Stix J. & Williams S.N.
719 1994. Correlations between SO₂ Flux and Long-Period Seismicity at Galeras Volcano. *Nature*
720 **368** (135-137).
721
- 722 FOROOZAN R., ELSWORTH D., VOIGHT B. & MATTIOLI G.S. 2010. Dual reservoir structure at
723 Soufriere Hills Volcano inferred from continuous GPS observations and heterogeneous elastic
724 modeling. *Geophysical Research Letters* **37**. doi: 10.1029/2010GL042511.
725
- 726 FOROOZAN R., ELSWORTH D., VOIGHT B. & MATTIOLI G.S. 2011. Magmatic-metering controls
727 the stopping and restarting of eruptions. *Geophysical Research Letters* **38**. L05306, doi:
728 10.1029/2010GL046591.
729
- 730 GALLE B., OPPENHEIMER C., GEYER A., MCGONIGLE A.J.S., EDMONDS M. & HORROCKS L.
731 2003. A miniaturised ultraviolet spectrometer for remote sensing of SO₂ fluxes: a new tool for
732 volcano surveillance. *Journal of Volcanology and Geothermal Research* **119**(1-4), 241-254.
733
- 734 GARDNER C.A. & WHITE R.A. 2002. Seismicity, gas emission and deformation from 18 July to
735 25 September 1995 during the initial phreatic phase of the eruption of Soufrière Hills Volcano,
736 Montserrat *Geological Society, London, Memoirs* **21** (1), 567-581
737
- 738 GERLACH T.M. & MCGEE K.A. 1994 Total sulfur dioxide emissions and pre-eruption vapor-
739 saturated magma at Mount St. Helens, 1980-88. *Geophysical. Research. Letters* **21**(25), 2833-
740 2836.
741
- 742 HARRIS A.J.L. & NERI M. 2002. Volumetric observations during paroxysmal eruptions at Mount
743 Etna: pressurized drainage of a shallow chamber or pulsed supply? *Journal of Volcanology and*
744 *Geothermal Research* **116**(1-2), 79-95.
745
- 746 HARRIS A., DEHN J., PATRICK M., CALVARI S., RIPEPE M. & LODATO L. 2005. Lava effusion
747 rates from hand-held thermal infrared imagery: an example from the June 2003 effusive activity
748 at Stromboli. *Bulletin of Volcanology* **68**(2), 107-117.
749
- 750 HERD R.A., EDMONDS M. & BASS V.A. 2005. Catastrophic lava dome failure at Soufrière Hills
751 Volcano, Montserrat, 12-13 July 2003. *Journal of Volcanology and Geothermal Research* **148**
752 (3-4), 234-252.
753
- 754 HIRABAYASHI J., OHBA T., NOGAMI K. & YOSHIDA M. 1995. Discharge Rate of SO₂ from Unzen
755 Volcano, Kyushu, Japan. *Geophysical Research Letters* **22**(13), 1709-1712.
756
- 757 HUMPHREYS M.C.S., CHRISTOPHER T. & HARDS V. 2009. Microlite transfer by disaggregation of
758 mafic inclusions following magma mixing at Soufriere Hills volcano, Montserrat. *Contributions*
759 *to Mineralogy and Petrology* **157**(5), 609-624.
760
- 761 HUMPHREYS M.C.S., EDMONDS M., CHRISTOPHER T. & HARDS V. 2009. Chlorine variations in
762 the magma of Soufriere Hills Volcano, Montserrat: Insights from Cl in hornblende and melt
763 inclusions. *Geochimica Et Cosmochimica Acta* **73**(19), 5693-5708.

- 764 HUMPHREYS M.C.S., EDMONDS M., BARCLAY J., PLAIL M., PARKES D. & CHRISTOPHER T. 2012.
765 A new method to quantify the real supply of mafic components to a hybrid andesite.
766 *Contributions to Mineralogy and Petrology* 65 (1) 191-215
767
- 768 KARLSTROM L., DUFEK J. & MANGA M. 2010. Magma chamber stability in arc and continental
769 crust. *Journal of Volcanology and Geothermal Research* **190**(3-4), 249-270.
770
- 771 KAZAHAYA K., SHINOHARA H. & SAITO G. (1994). Excessive Degassing of Izu-Oshima
772 Volcano Magma Convection in a Conduit. *Bulletin of Volcanology* **56**(3), 207-216.
773
- 774 KENT A.J.R., DARR C., KOLESZAR A.M., SALISBURY M.J. & COOPER K.M. 2010. Preferential
775 eruption of andesitic magmas through recharge filtering. **3**(9), 631-636.
776
- 777 KOMOROWSKI J.C., LEGENDRE Y., CHRISTOPHER T., BERNSTEIN M., STEWART R., JOSEPH E.,
778 FOURNIER N., CHARDOT L., FINIZOLA A., WADGE G., SYERS R., WILLIAMS C. & BASS V. 2010.
779 Insights into processes and deposits of hazardous vulcanian explosions at Soufriere Hills
780 Volcano during 2008 and 2009 (Montserrat, West Indies). *Geophysical Research Letters* **37**.
781 L00E19, doi: 10.1029/2010GL042558.
782
- 783 KRESS V. 1997. Magma mixing as a source for Pinatubo sulphur. **389**(6651), 591-593.
784
- 785 LAUTZE N.C., HARRIS A.J.L., BAILEY J.E., RIPEPE M., CALVARI S., DEHN J., ROWLAND S.K. &
786 Evans-Jones K. 2004. Pulsed lava effusion at Mount Etna during 2001. *Journal of Volcanology*
787 *and Geothermal Research* **137**(1-3): 231-246.
788
- 789 LENSKY N.G., SPARKS R.S.J., NAVON O. & LYAKHOVSKY V. 2008. Cyclic activity at Soufrière
790 Hills Volcano, Montserrat: degassing-induced pressurization and stick-slip extrusion
791 *Geological Society, London, Special Publications* **307** (1), 169-188
792
- 793 LINDE A.T., SACKS S., HIDAYAT D., VOIGHT B., CLARKE A., ELSWORTH D., MATTIOLI G.,
794 MALIN P., SHALEV E., SPARKS S. & WIDIWIJAYANTI C. 2010. Vulcanian explosion at Soufrière
795 Hills Volcano, Montserrat on March 2004 as revealed by strain data. *Geophysical Research*
796 *Letters* **37**(19), L00E07.
797
- 798 LOUGHLIN S.C., LUCKETT R., RYAN G., CHRISTOPHER T., HARDS V., De ANGELIS S., JONES L.
799 & STRUTT M. 2010. An overview of lava dome evolution, dome collapse and cyclicity at
800 Soufrière Hills Volcano, Montserrat, 2005 -2007. *Geophysical. Research. Letters*. **37**: L00E16.
801 doi: 10.1029/2010GL042547
802
- 803 LUCKETT R., BAPTIE B. & NEUBERG J. 2002. The relationship between degassing and rockfall
804 signals at Soufriere Hills Volcano, Montserrat. *Geological Society, London, Memoirs* **21**(1), 595-
805 602.
806
- 807 MARTEL C., RADADI Ali, A., POUSSINEAU S., GOURGAUD A. & PICHAVANT M. 2006. Basalt-
808 inherited microlites in silicic magmas: Evidence from Mount Pelée (Martinique, French West
809 Indies) *Geology* **34**(11): 905-908.

- 810 MARTIN V.M., HOLNESS M.B. & PYLE D.M. 2006. Textural analysis of magmatic enclaves from
811 the Kameni Islands, Santorini, Greece. *Journal of Volcanology and Geothermal Research* **154**(1-
812 2), 89-102.
- 813
814 McGEE K.A. & SUTTON, A.J. 1994. Eruptive activity at Mount St Helens, Washington, USA,
815 1984-1988: a gas geochemistry perspective. *Bulletin of Volcanology*, **56** (435-446).
816
- 817 MCGONIGLE A.J.S., OPPENHEIMER C., HAYES A.R., GALLE B., EDMONDS M., CALTABIANO T.,
818 SALERNO G., BURTON M. & MATHER T.A. 2003. Sulphur dioxide fluxes from Mount Etna,
819 Vulcano, and Stromboli measured with an automated scanning ultraviolet spectrometer. *Journal*
820 *of Geophysical Research: Solid Earth* **108**(B9): 2455.
821
- 822 MELNIK O. & COSTA A. 2014. Dual chamber-conduit models of non-linear dynamics behaviour
823 at Soufrière Hills Volcano, Montserrat. *Geological Society of London Memoir*, eds. G. Wadge,
824 R. Robertson, B. Voight, The eruption of Soufrière Hills Volcano, Montserrat from 2000 to
825 2010.
- 826 MELNIK O. & SPARKS R.S.J. 1999. Nonlinear dynamics of lava dome extrusion *Nature* **402** (37-
827 41) doi:10.1038/46950
- 828 MELNIK O. & SPARKS R.S.J. 2002. Dynamics of magma ascent and lava extrusion at Soufrière
829 Hills Volcano, Montserrat. *Geological Society, London, Memoirs* **21**(1), 153-171.
830
- 831 MELNIK O. & SPARKS R.S.J. 2005. Controls on conduit magma flow dynamics during lava
832 dome building eruptions. *Journal of Geophysical Research: Solid Earth* **110**(B2): B02209.
833
- 834 MILLER A.D., STEWART R.C., WHITE R.A., LUCKETT R., BAPTIE B.J., ASPINALL W.P.,
835 LATCHMAN J.L., LYNCH L.L. & VOIGHT B. 1998. Seismicity associated with dome growth and
836 collapse at the Soufriere Hills Volcano, Montserrat. *Geophysical. Research. Letters*. **25**(18),
837 3401-3404.
838
- 839 MORETTI, R. & PAPALE, P. 2004. On the oxidation state and volatile behavior in multicomponent
840 gas -melt equilibria. *Chemical Geology* **213**(1-3), 265-280.
841
- 842 MURPHY M.D., SPARKS R.S.J., BARCLAY J., CARROLL M.R. & BREWER T.S. 2000.
843 Remobilization of andesite magma by intrusion of mafic magma at the Soufriere Hills Volcano,
844 Montserrat, West Indies. *Journal of Petrology* **41**(1), 21-42.
845
- 846 MURPHY M.D., SPARKS R.S.J., BARCLAY J., CARROLL M.R., LEJEUNE A.M., BREWER T.S.,
847 MACDONALD R., BLACK S. & YOUNG S. (1998). The role of magma mixing in triggering the
848 current eruption at the Soufriere Hills volcano, Montserrat, West Indies. *Geophysical Research*
849 *Letters* **25**(18): 3433-3436.
850
851

- 852 Nicholson E.J., Mather T.A., Pyle D.M., Odbert H.M. & Christopher T. 2013. Cyclical patterns
853 in volcanic degassing revealed by SO₂ flux timeseries analysis: An application to Soufrière Hills
854 Volcano, Montserrat. *Earth and Planetary Science Letters* **375** (0), 209-221.
855
- 856 NORTON G.E., WATTS R.B., VOIGHT B., MATTIOLI G.S., HERD R.A., YOUNG S.R., DEVINE G.E.,
857 ASPINNALL W.P., BONADONNA C., BAPTIE B.J., EDMONDS M., JOLLY A.D., LOUGHLIN S.C.,
858 LUCKETT R. & SPARKS S.J. 2002. Pyroclastic flow and explosive activity at Soufriere Hills
859 Volcano, Montserrat, during a period of virtually no magma extrusion (March 1998 to November
860 1999) *Geological Society, London, Memoirs* **21**(1), 467-481.
861
- 862 ODBERT H.M., STEWART R.C & WADGE G. 2014. Cyclic phenomena at Soufriere Hills Volcano,
863 Montserrat. *Geological Society of London Memoir*, eds. G. Wadge, R. Robertson, B. Voight, The
864 eruption of Soufrière Hills Volcano, Montserrat from 2000 to 2010.
865
- 866 OHBA T., HIRABAYASHI J., NOGAMI K., KUSAKABE M. & YOSHIDA M. 2008. Magma degassing
867 process during the eruption of Mt. Unzen, Japan in 1991 to 1995: Modeling with the chemical
868 composition of volcanic gas. *Journal of Volcanology and Geothermal Research*
869 *Scientific drilling at Mount Unzen* **175**(1-2), 120-132.
870
- 871 OPPENHEIMER C., FRANCIS P. & STIX J. 1998. Depletion rates of sulfur dioxide in tropospheric
872 volcanic plumes. *Geophysical Research Letters* **25**(14), 2671-2674.
873
- 874 OPPENHEIMER C., LOMAKINA A.S., KYLE P.R., KINGSBURY N.G. & BOICHU M. 2009. Pulsatory
875 magma supply to a phonolite lava lake. *Earth and Planetary Science Letters* **284**(3-4), 392-398.
876
- 877 PAULATTO M., ANNEN C., HENSTOCK T.J., KIDDLE E.J., MINSHULL T.A., SPARKS R.S.J. &
878 VOIGHT B. 2011. Magma chamber properties from integrated seismic tomography and thermal
879 modeling at Montserrat. *Geochemistry Geophysics Geosystems* **13** (1),
880 doi:10.1029/2011GC003892
881
- 882 PAULATTO M., MINSHULL T.A., BAPTIE B., DEAN S., HAMMOND J.O.S., HENSTOCK T., KENEDI
883 C.L., KIDDLE E.J., MALIN P., PEIRCE C., RYAN G., SHALEV E., SPARKS R.S.J. & VOIGHT B.
884 2010. Upper crustal structure of an active volcano from refraction/reflection tomography,
885 Montserrat, Lesser Antilles *Geophysical Journal International* **180** (2): 685-696
886
- 887 Percival D. & Walden A. 2000. Wavelet Methods for Time Series Analysis (Cambridge Series in
888 Statistical and Probabilistic Mathematics), Cambridge University Press.
889
- 890 PHILLIPS J.C. & WOODS A.W. 2002. Suppression of large-scale magma mixing by melt-volatile
891 separation. *Earth and Planetary Science Letters* **204**(1-2), 47-60.
892
- 893 PLAIL M., BARCLAY J., HUMPHREYS M.C.S., EDMONDS M., HERD R.A. & CHRISTOPHER T. 2012.
894 Characterisation of mafic enclaves in the erupted products of Soufrière Hills Volcano,
895 Montserrat 1995-2010. *Geological Society of London Memoir*, eds. G. Wadge, R. Robertson, B.
896 Voight, The eruption of Soufrière Hills Volcano, Montserrat from 2000 to 2010.
897

- 898 PLATT U. 1994. Differential optical absorption spectroscopy (DOAS). *Air Monitoring by*
899 *Spectroscopic Technique* **127**: 27-84.
900
- 901 ROBERTSON R.E.A., ASPINALL W.P., HERD R.A., NORTON G.E., SPARKS R.S.J. & YOUNG S.R.
902 2000. The 1995-1998 eruption of the Soufriere Hills volcano, Montserrat, WI. *Philosophical*
903 *Transactions of the Royal Society of London Series a-Mathematical Physical and Engineering*
904 *Sciences* **358**(1770), 1619-1637.
905
- 906 RODRIGUEZ L.A., WATSON I.M., EDMONDS M., RYAN G., HARDS V., OPPENHEIMER C.M.M. &
907 BLUTH G.J.S. 2008. SO₂ loss rates in the plume emitted by Soufriere Hills volcano, Montserrat.
908 *Journal of Volcanology and Geothermal Research* **173**(1-2), 135-147.
909
- 910 Ruprecht, P. and Plank, T. (2013). "Feeding andesitic eruptions with a high-speed connection
911 from the mantle." **500**(7460): 68-72.
912
- 913 RUTHERFORD M.J. & DEVINE J.D. 2003. Magmatic Conditions and Magma Ascent as Indicated
914 by Hornblende Phase Equilibria and Reactions in the 1995-2002 Soufrière Hills Magma. *Journal*
915 *of Petrology* **44**(8), 1433-1453.
916
- 917 RYAN G.A., LOUGHLIN S.C., JAMES M.R., JONES L.D., CALDER E.S., CHRISTOPHER T., STRUTT
918 M.H. & WADGE G. 2010. Growth of the lava dome and extrusion rates at Soufriere Hills
919 Volcano, Montserrat, West Indies: 2005-2008. *Geophysical Research Letters* **37**. L00E08, doi:
920 10.1029/2009GL041477.
921
- 922 SATO H., NAKADA S., FUJII T., NAKAMURA M. & SUZUKI-KAMATA K. 1999. Groundmass
923argasite in the 1991-1995 dacite of Unzen volcano: phase stability experiments and
924 volcanological implications. *Journal of Volcanology and Geothermal Research* **89**(1-4), 197-
925 212.
926
- 927 SATO H., HOLTZ F., BEHRENS H., BOTCHARNIKOV R. & NAKADA S. 2005. Experimental
928 Petrology of the 1991-1995 Unzen Dacite, Japan. Part II: Cl/OH Partitioning between
929 Hornblende and Melt and its Implications for the Origin of Oscillatory Zoning of Hornblende
930 Phenocrysts. *Journal of Petrology* **46**(2), 339-354.
- 931 Scaillet B. & Pichavant M. 2005. A model of sulphur solubility for hydrous mafic melts:
932 application to the determination of magmatic fluid compositions of Italian volcanoes. *Annals of*
933 *Geophysics*. **48** (4-5) 671-698.
934
- 935 Scaillet B., Clemente B., Evans B.W. & Pichavant M. 1998. Redox control of sulfur degassing in
936 silicic magmas. *Journal of Geophysical Research*. **103**(B10): 23937-23949.
937
- 938 SHINOHARA H. 2008. Excess Degassing from Volcanoes and Its Role on Eruptive and Intrusive
939 Activity. *Reviews of Geophysics* **46**(4). doi:10.1029/2007RG000244.
940
941

- 942 SHINOHARA H., OHBA T., KAZAHAYA K. & TAKAHASHI H. 2008. Origin of volcanic gases
943 discharging from a cooling lava dome of Unzen volcano, Japan. *Journal of Volcanology and*
944 *Geothermal Research* **175**(1-2), 133-140.
- 945
946 SPARKS R.S.J. & YOUNG S.R. 2002. The eruption of Soufriere Hills Volcano, Montserrat (1995-
947 1999): overview of scientific results. *Geological Society, London, Memoirs* **21**(1), 45-69.
- 948
949
950 SPARKS R.S.J. 2003. Dynamics of magma degassing. *Geological Society, London, Special*
951 *Publications*. **213**(1). 5-22
- 952
953
954 STEVENSON, D.S. & BLAKE, S. 1998. Modelling the dynamics and thermodynamics of volcanic
955 degassing. *Bulletin of Volcanology* **60**(4), 307-317.
- 956
957 STINTON A.J., COLE P.D., ODBERT H.M., CHRISTOPHER T.E., AVARD G. & BERNSTEIN M. 2014.
958 Evolution of the Soufrière Hills volcano during a short, intense episode of dome growth: 4
959 October 2009 - 11 February 2010. *Geological Society of London Memoir*, eds. G. Wadge, R.
960 Robertson, B. Voight, The eruption of Soufrière Hills Volcano, Montserrat from 2000 to 2010.
- 961
962 STOIBER R.E., WILLIAMS S.N. & HUEBERT B. 1987. Annual contribution of sulfur dioxide to the
963 atmosphere by volcanoes. *Journal of Volcanology and Geothermal Research* **33**(1-3), 1-8.
- 964
965 SWEENEY D., KYLE P.R. & OPPENHEIMER C. 2008. Sulfur dioxide emissions and degassing
966 behavior of Erebus volcano, Antarctica. *Journal of Volcanology and Geothermal Research*
967 **177**(3), 725-733.
- 968
969 TAISNE B. & JAUPART C. 2008. Magma degassing and intermittent lava dome growth.
970 *Geophysical Research Letters* **35**(20). L20310, doi: 10.1029/2008GL035432.
- 971
972 TOMIYA A., TAKAHASHI E., FURUKAWA N. & SUZUKI T. 2010. Depth and Evolution of a Silicic
973 Magma Chamber: Melting Experiments on a Low-K Rhyolite from Usu Volcano, Japan. *Journal*
974 *of Petrology* **51** (6), 1333-1354
- 975
976 TORRENCE C. & COMPO G.P. 1998. A Practical Guide to Wavelet Analysis. *Bulletin of the*
977 *American Meteorological Society* **79**(1), 61-78.
- 978
979 VOIGHT B., CONSTANTINE E.K., SISWOWIDJOYO S. & TORLEY, R. 2000. Historical eruptions of
980 Merapi Volcano, Central Java, Indonesia, 1768-1998. *Journal of Volcanology and Geothermal*
981 *Research* **100**(1-4), 69-138.
- 982
983 VOIGHT B., HOBLITT R. P., CLARKE A. B., LOCKHART A. B., MILLER A. D., LYNCH L. &
984 MCMAHON J. 1998. Remarkable cyclic ground deformation monitored in real-time on
985 Montserrat, and its use in eruption forecasting. *Geophysical Research Letters* **25** (18) 3405-3408
986 doi: 10.1029/98GL01160
- 987

- 988 VOIGHT B., SPARKS R.S.J., MILLER A.D., STEWART R.C., HOBLITT R.P., CLARKE A., EWART J.,
989 ASPINALL W.P., BAPTIE B., CALDER E.S., COLE P., DRUITT T.H., HARTFORD C., HERD R.A.,
990 JACKSON P., LEJEUNE A.M., LOCKHART A.B., LOUGHLIN S.C., LUCKETT R., LYNCH L., NORTON
991 G.E., ROBERTSON R., WATSON I.M., WATTS R. & YOUNG S.R. 1999. Magma flow instability
992 and cyclic activity at Soufriere Hills Volcano, Montserrat, British West Indies. *Science*
993 **283**(5405), 1138-1142.
994
- 995 WADGE G., HERD R., RYAN G., CALDER E.S. & KOMOROWSKI J.C. 2010. Lava production at
996 Soufriere Hills Volcano, Montserrat: 1995-2009. *Geophysical Research Letters* **37**. L00E03,
997 doi:10.1029/2009GL041466.
998
- 999 WALLACE P.J. 2001. Volcanic SO₂ emissions and the abundance and distribution of exsolved gas
1000 in magma bodies. *Journal of Volcanology and Geothermal Research* **108**(1-4), 85-106.
1001
- 1002 WALLACE P.J. 2005. Volatiles in subduction zone magmas: concentrations and fluxes based on
1003 melt inclusion and volcanic gas data. *Journal of Volcanology and Geothermal Research* **140**(1-
1004 3), 217-240.
1005
- 1006 WALLACE P.J. & GERLACH T.M. 1994. Magmatic Vapor Source for Sulfur Dioxide Released
1007 During Volcanic Eruptions: Evidence from Mount Pinatubo. *Science* **265** (497-499).
1008
- 1009 WALLACE P.J. & EDMONDS M. 2011. The Sulfur Budget in Magmas: Evidence from Melt
1010 Inclusions, Submarine Glasses, and Volcanic Gas Emissions. *Reviews in Mineralogy and*
1011 *Geochemistry* **73** (1), 215-246
1012
- 1013 WATSON I.M., OPPENHEIMER C., VOIGHT B., FRANCIS P., CLARKE A., STIX J., MILLER A., PYLE
1014 D.M., BURTON M.R., YOUNG S.R., NORTON G., LOUGHLIN S., DARROUX B. & STAFF M.V.O.
1015 2000. The relationship between degassing and ground deformation at Soufriere Hills Volcano,
1016 Montserrat. *Journal of Volcanology and Geothermal Research* **98**(1-4), 117-126.
1017
- 1018 WERNER C., CHRISTENSON B.W., HAGERTY M. & BRITTEN K. 2006. Variability of volcanic gas
1019 emissions during a crater lake heating cycle at Ruapehu Volcano, New Zealand. *Journal of*
1020 *Volcanology and Geothermal Research* **154**(3-4), 291-302.
1021
- 1022 WERNER C., EVANS W.C., KELLY P.J., MCGIMSEY R., PFEFFER M., DOUKAS M. & NEAL C.
1023 2012. Deep magmatic degassing versus scrubbing: Elevated CO₂ emissions and C/S in the lead-
1024 up to the 2009 eruption of Redoubt Volcano, Alaska. *Geochemistry, Geophysics, Geosystems*
1025 **13**(3), doi: 10.1029/2011GC003794.
1026
- 1027 WERNER C., KELLY P.J., DOUKAS M., LOPEZ T., PFEFFER M., MCGIMSEY R. & NEAL C. 2013.
1028 Degassing of CO₂, SO₂, and H₂S associated with the 2009 eruption of Redoubt Volcano, Alaska.
1029 *Journal of Volcanology and Geothermal Research* **259**(0), 270-284.
1030
- 1031 WESTRICH, H.R. & GERLACH, T.M. (1992). Magmatic gas source for the stratospheric SO₂ cloud
1032 from the June 15, 1991, eruption of Mount Pinatubo. *Geology* **20** (10), 867-870
1033

- 1034 WITHAM F. 2011. Conduit convection, magma mixing, and melt inclusion trends at persistently
1035 degassing volcanoes. *Earth and Planetary Science Letters* **301**(1-2), 345-352.
1036
- 1037 YOUNG S.R., VOIGHT B. & DUFFELL H.J. 2003. Magma extrusion dynamics revealed by high-
1038 frequency gas monitoring at Soufriere Hills Volcano, Montserrat. *Volcanic Degassing* **213** (219-
1039 230).
1040
- 1041 YOUNG S.R., SPARKS R.S.J., ASPINALL W.P., LYNCH L.L., MILLER A.D., ROBERTSON R.E.A. &
1042 SHEPHERD J.B. 1998. Overview of the eruption of Soufriere Hills Volcano, Montserrat, 18 July
1043 1995 to December 1997. *Geophysical Research. Letters* **25**(18), 3389-3392.
1044
- 1045 YOUNG S.R., FRANCIS P.W., BARCLAY J., CASADEVALL T.J., GARDNER C.A., DARROUX B.,
1046 DAVIES M.A., DELMELLE P., NORTON G.E., MACIEJEWSKI A.J.H., OPPENHEIMER C.M.M., STIX
1047 J. & WATSON I.M. (1998). Monitoring SO₂ emission at the Soufriere Hills Volcano: Implications
1048 for changes in eruptive conditions. *Geophysical. Research. Letters* **25**(19), 3681-3684.
1049
- 1050 ZELLMER G.F., SPARKS R.S.J., HAWKESWORTH C.J. & WIEDENBECK, M. 2003. Magma
1051 Emplacement and Remobilization Timescales Beneath Montserrat: Insights from Sr and Ba
1052 Zonation in Plagioclase Phenocrysts. *Journal of Petrology* **44**(8), 1413-1431.
- 1053 ZOBIN V.M., VARLEY N.R., GONZÁLEZ M., OROZCO J., REYES G.A., NAVARRO C. & BRETÓN M.
1054 2008. Monitoring the 2004 andesitic block-lava extrusion at Volcan de Colima, Mexico from
1055 seismic activity and SO₂ emission. *Journal of Volcanology and Geothermal Research* **177**(2),
1056 367-377.
1057

Tables

Pulse/Int	Mean flux t/d	# of values	% Data Obtained	Approximate duration/ yrs
1st Int (June 2004 – April 2005)	427	250	69	0.99
2nd Int (Jul 2006 – Jul 2007)	304	317	92	0.94
1st pulse (June 2002 – May 2004)	561	625	86	2
2nd pulse (April 2005 – Jul 2006)	560	435	76	1.58
3 rd pulse (Jul 2nd 2007 - Jan 2010)*	664	732	87	2.31
2010 restart (mid march) - present	401	1040	82	3.47

Table 1 Break down of the relevant parameters of the pulses and intermediate periods that were observed in the uv network data. * denotes pulse where data was lost due to ash from Phase V

Figures

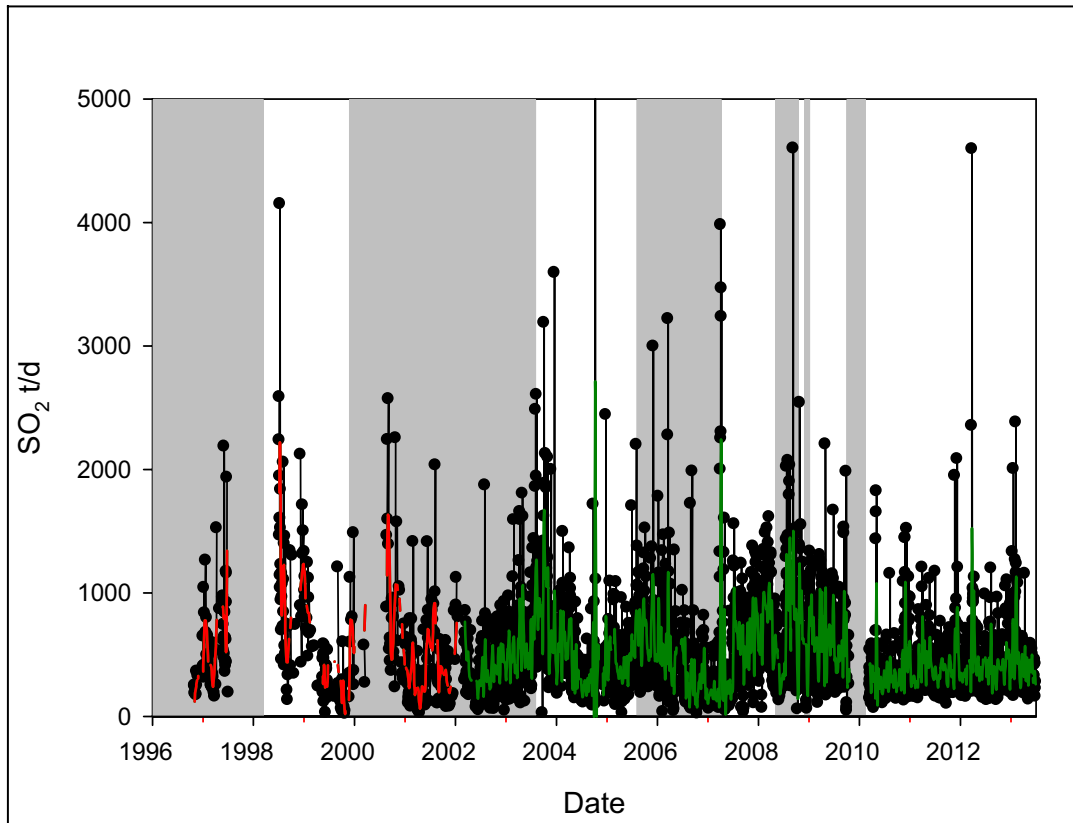


Figure 1 The Entire SO₂ time series showing continuous and variable SO₂ output throughout the eruption. Red line is 11 day filter through the COSPEC data and green line if 11 day filter through the spectrometer network data.



Figure 2 Google Earth image of southern Montserrat showing the location of the two network spectrometers relative to the volcano. The spectrometers are named based on their location (LL – Lovers lane, BR – Brodericks) . The prevailing winds are easterlies which normally puts the plume over Plymouth. In this image the plume is to the north of the network.

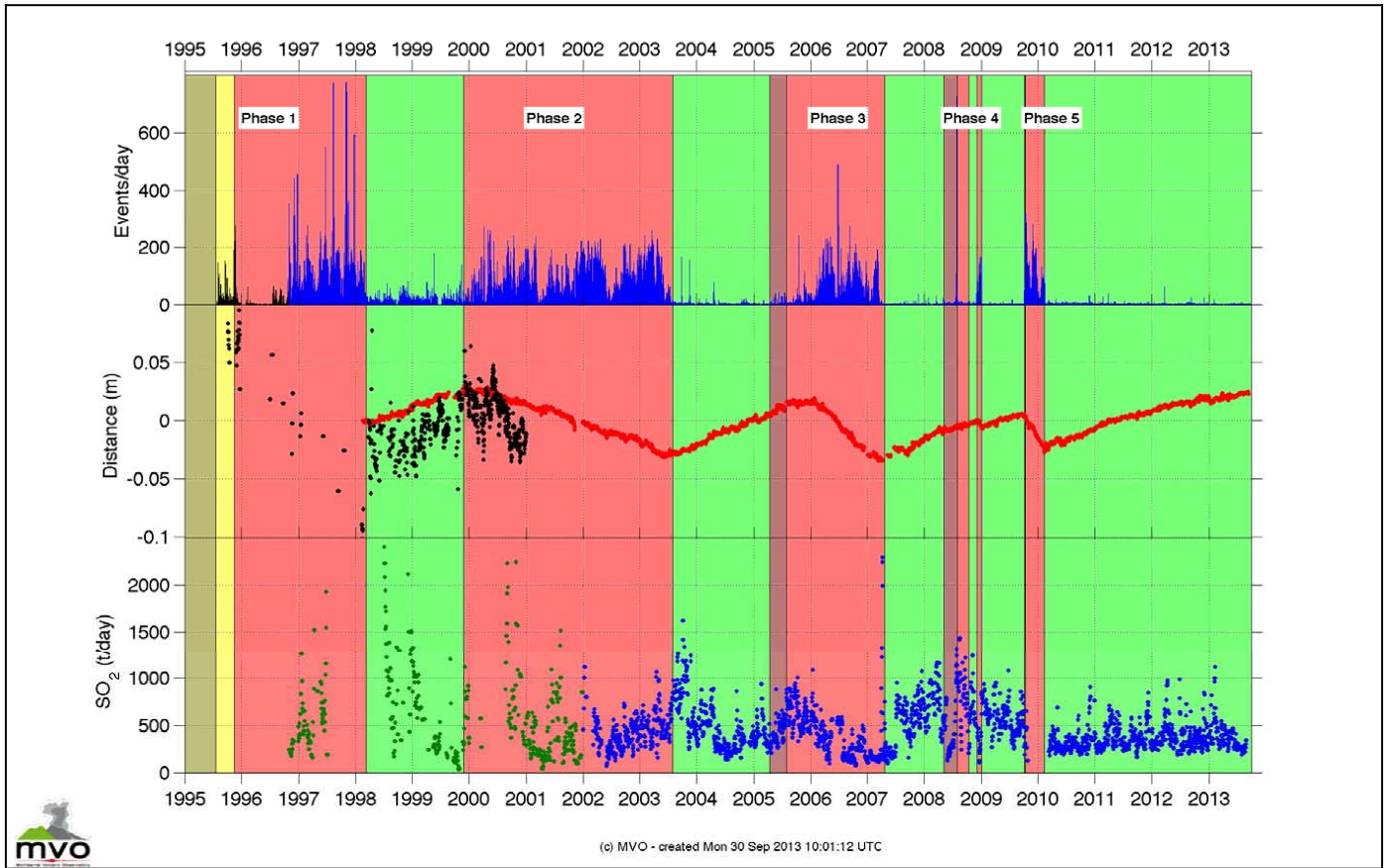


Figure 3 Multi-plot diagram used by the MVO showing how the seismic (top), deformation (middle) and SO₂ varied throughout the whole eruption

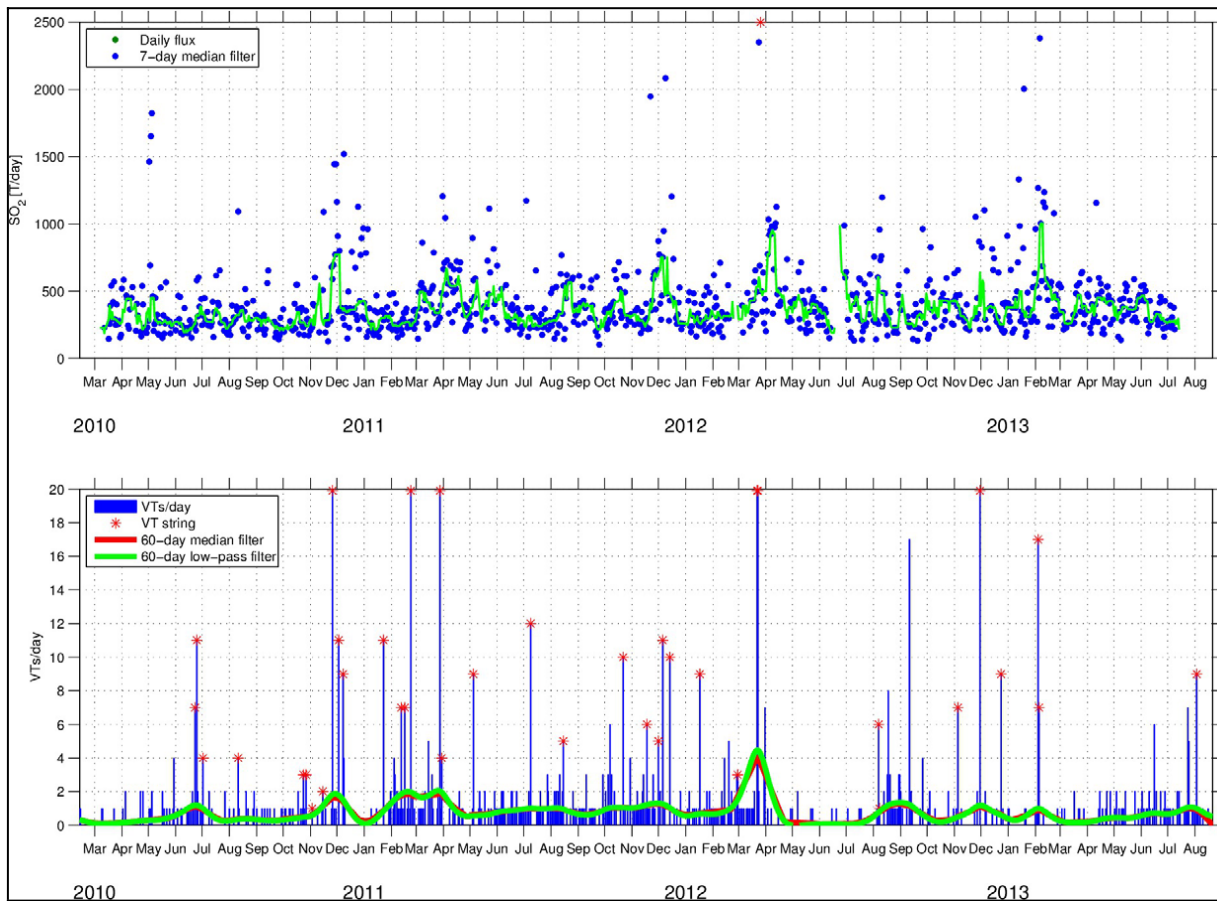


Figure 4 A comparison of mean daily post Phase V SO_2 flux values with VT earthquakes showing a fairly good correlation

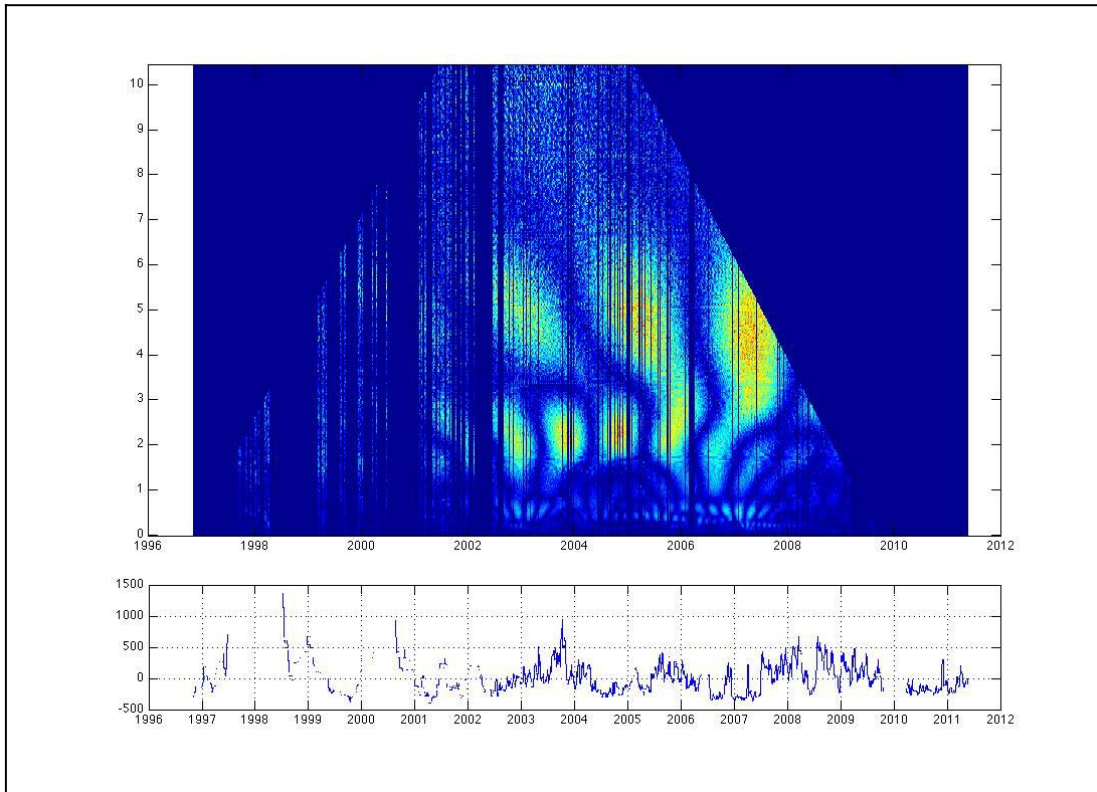


Figure 5 wavelet plot of the whole SO₂ dataset showing the ~ 2 year signal in the time series.

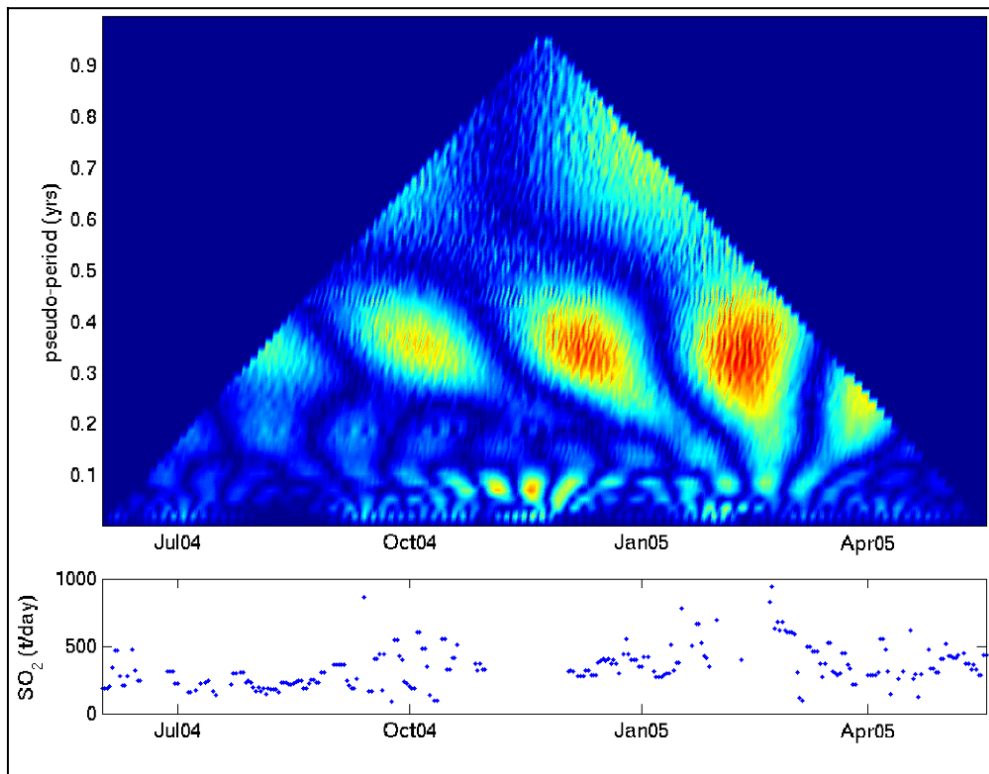


Figure 6 Wavelet plot of the SO₂ data from 2004 – 2005 showing the ~ 5 month cycle occurring during the second pause

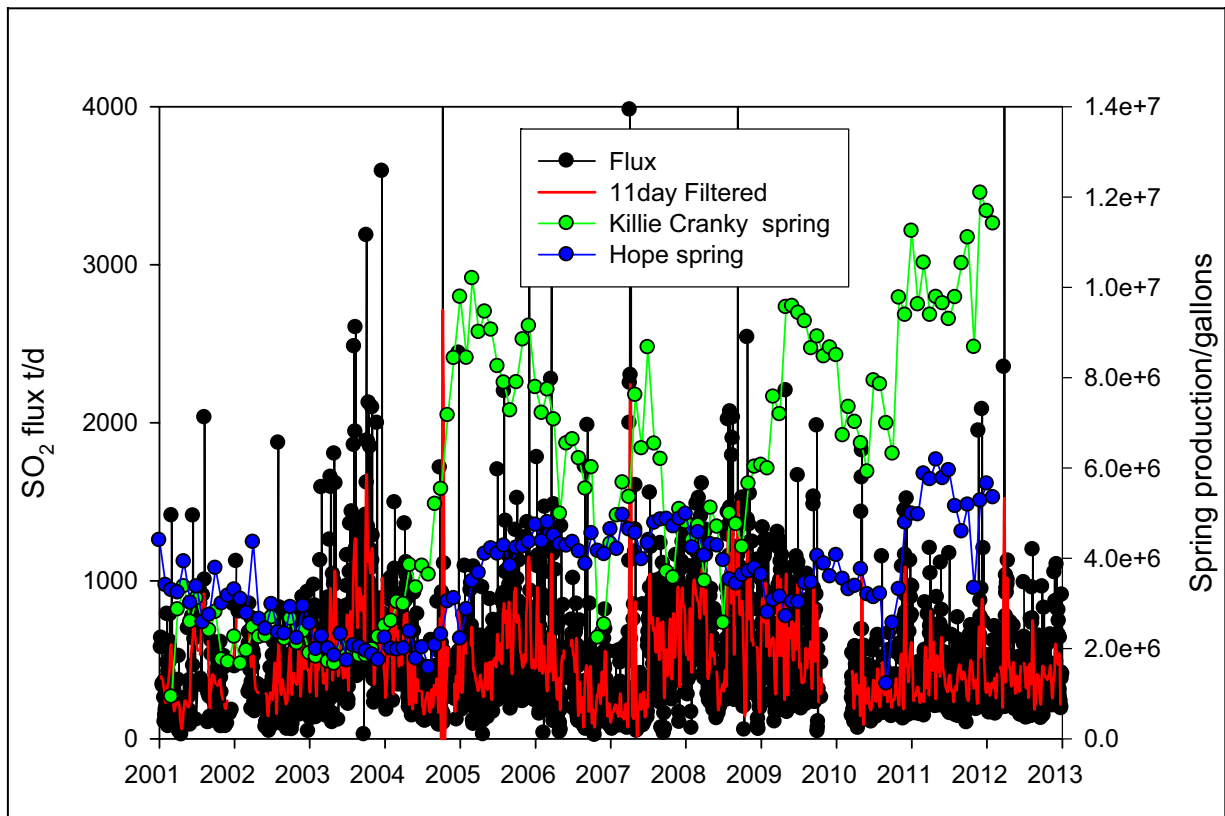


Figure 7 Comparisons of UV network flux data with production data from two center hills springs from 2001 till present

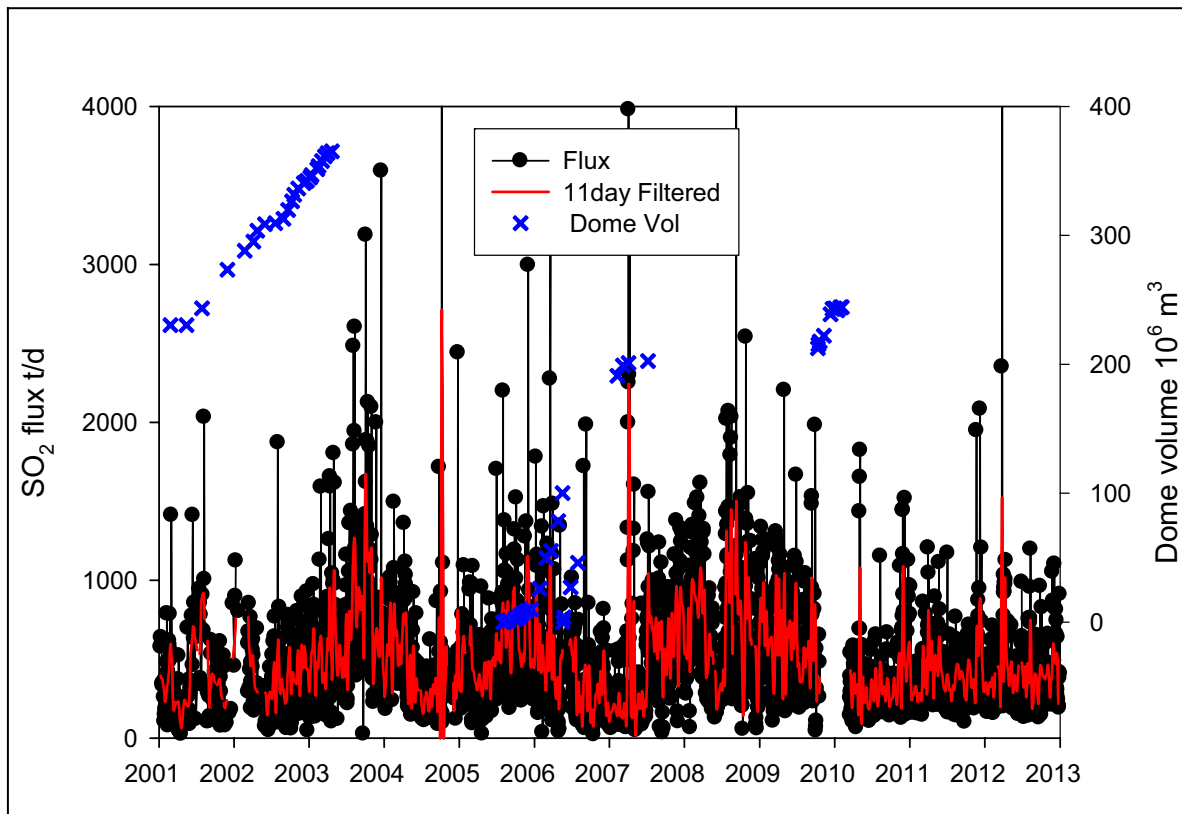


Figure 8 A comparison of dome volume and SO₂ flux from 2001 till present.

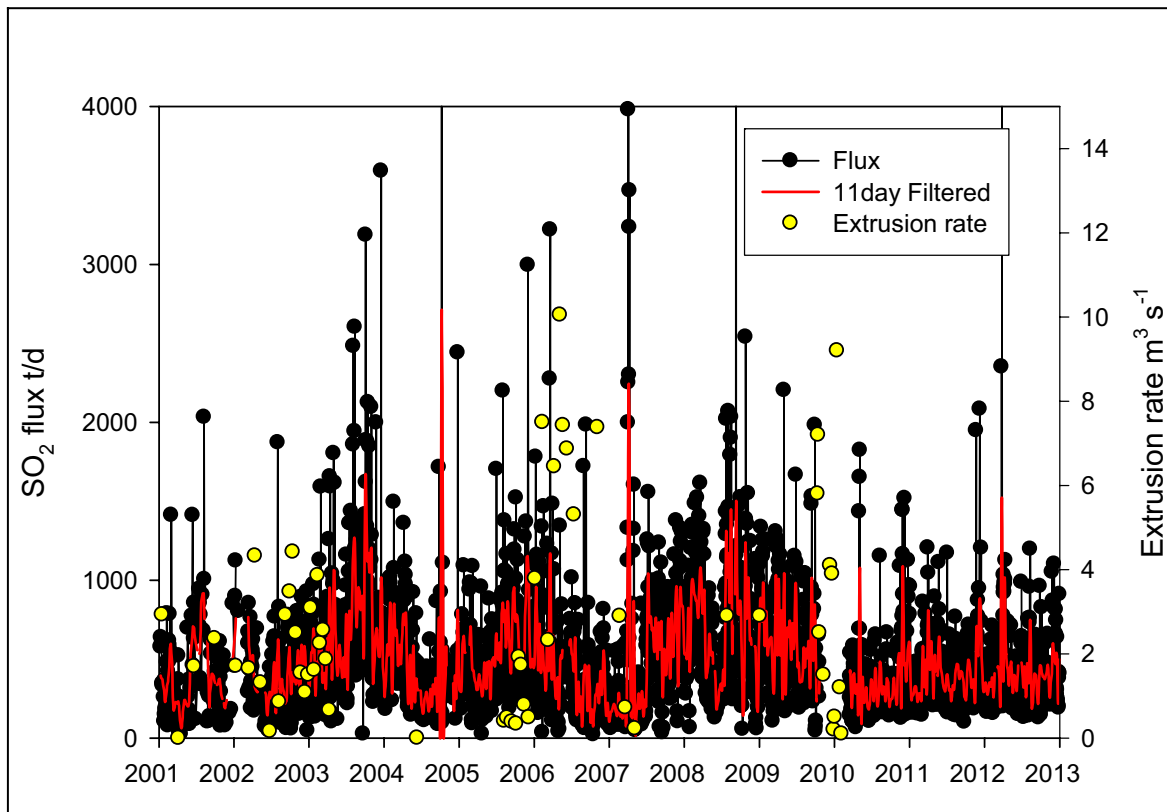


Figure 9 Andesite extrusion rate compared to daily SO₂ flux rates from 2001 till present